Effect of Postmortem Time and Preservation Fluid on the Tensile Material Properties of Bovine Liver Parenchyma

Kristin Marie Dunford

Thesis submitted to the faculty of the
Virginia Polytechnic Institute and State University
in partial fulfillment of the requirements for the degree of

Master of Science
In
Biomedical Engineering

Andrew R. Kemper, Chair
Warren N. Hardy
Stefan M. Duma

October 5, 2017
Blacksburg, Virginia

Keywords: Liver, Bovine, Failure, Tension, Stress, Strain, Postmortem

Effect of Postmortem Time and Preservation Fluid on the Tensile Material Properties of Bovine Liver Parenchyma

Kristin Marie Dunford

Academic Abstract

The liver is one of the most frequently injured abdominal organs in motor vehicle collisions. Although previous studies have quantified the tensile failure properties of human liver parenchyma at 48hrs postmortem, it is currently unknown how the material properties change between time of death and 48hrs postmortem. Therefore, the purpose of this study was to quantify the effects of postmortem degradation on the tensile material properties of bovine liver parenchyma when stored in DMEM or saline. Fourteen fresh bovine livers were obtained from a local slaughter house and stored in either DMEM or saline as large blocks, small blocks, or slices of tissue. Multiple parenchyma dog-bone samples from each liver were tested once to failure at three time points: ~6hrs, ~24hrs, and ~48hrs postmortem. The data were then analyzed to determine if there were significant changes in the material properties with respect to postmortem time. The results showed that the failure strain decreased significantly between 6hrs and 48hrs after death when stored as large blocks in saline. Conversely, neither the failure stress nor failure strain changed significantly with respect to postmortem time when stored as large blocks in DMEM. The modulus did not significantly change for tissue stored as large blocks in either fluid. Preliminary results indicated that reducing the tissue storage size had a negative effect on the material properties and cellular architecture. Overall, this study illustrated that the effects of postmortem liver degradation varied with respect to the preservation fluid, storage time, and storage block size.

Effect of Postmortem Time and Preservation Fluid on the Tensile Material Properties of Bovine Liver Parenchyma

Kristin Marie Dunford

General Audience Abstract

Although the liver is one of the most frequently injured abdominal organs in motor vehicle collisions (MVCs), currently accepted anthropomorphic test devices are unable to predict abdominal organ injury risk. Consequently, finite element models are becoming an important tool for assessing abdominal organ injury risk in MVCs. However, these models must be validated based on biomechanical data in order to accurately assess injury risk. Given that previous studies that have quantified the tensile failure properties of human liver parenchyma have been limited to testing at 48hrs postmortem, it is currently unknown how the material properties change between time of death and 48hrs postmortem. Therefore, the purpose of this study was to quantify the effects of postmortem degradation on the tensile material properties of bovine liver parenchyma with increasing postmortem time when stored in DMEM or saline. A total of 148 uniaxial tension tests were successfully conducted on parenchyma samples of fourteen bovine livers acquired immediately after death. Tissue was immersed in DMEM or saline and kept cool during preparation and storage. Twelve livers were stored as large blocks of tissue, while two livers were stored as small blocks and slices. Multiple dog-bone samples from each liver were tested once to failure at three time points: ~6hrs, ~24hrs, and ~48hrs after death. The data were then analyzed using a Linear Mixed Effect Model to determine if there were significant changes in the failure stress, failure strain, and modulus with respect to postmortem time. The results of the current study showed that the failure strain of bovine liver parenchyma decreased significantly between 6hrs and 48hrs after death when stored as large blocks in saline and refrigerated. Conversely, neither the failure stress nor failure strain changed significantly with respect to postmortem time when stored as large blocks in DMEM. The modulus did not significantly change for tissue stored as large blocks in either saline or DMEM. In addition, preliminary results indicated that reducing the tissue storage size had a negative effect on the material properties and cellular architecture. Overall, this study illustrated that the effects of postmortem liver degradation varied with respect to the preservation fluid, storage time, and storage block size.

ACKNOWLEDGEMENTS

Firstly, I am grateful to God, my husband, family, and friends for invaluable encouragement and support.

A special thank you to Dr. Tanya LeRoith for sharing her expertise and grading histology samples.

Thank you to Dr. Andrew Kemper for guidance throughout my graduate career. Also, thank you to Devon Albert, Valentina Heath, and all others not mentioned here, for support and assistance throughout all aspects of this study. Lastly, thanks to Dr. Warren Hardy and Dr. Stefan Duma for agreeing to be on my committee and providing feedback.

TABLE OF CONTENTS

LIST OF FIGURES

LIST OF TABLES

CHAPTER 1

INTRODUCTION

The liver is one of the most frequently injured abdominal organs in motor vehicle collisions (MVCs) (Lamielle et al., 2006; Yoganandan et al., 2000; Klinich et al., 2010). The liver's propensity for injury in blunt trauma is due to its large size, fixed position, and abundant vasculature (Malaki and Mangat, 2011). In a study using the Crash Injury Research and Engineering Network (CIREN), Holbrook et al. (2007) determined that of the 316 subjects with liver injury observed, 47% of the injuries were either moderate or major in severity. Furthermore, 81% of the injuries were lacerations. Similarly, Christmas et al. (2005) reported that 41% of all blunt hepatic injuries seen in a trauma registry were high grade injuries. For the high severity liver injuries that did not require operative management, the mortality was 2.2%. However, the mortality rate was 30% if operative management was necessary. Hurtuk et al. (2006) analyzed the National Trauma Data Bank and reported that the average overall liver injury mortality was 16.8% between 1994 and 2003.

Anthropomorphic testing devices (ATDs) and finite element models (FEMs) are frequently used to predict injury during MVCs. Despite the necessity to accurately predict abdominal organ injury risk, current ATDs lack the instrumentation necessary to represent individual organs (Hardy et al., 2015). In addition, the current frontal crash regulatory ATD, i.e., the Hybrid III, lacks a biofidelic abdomen (Hardy et al., 2015). Specifically, the Hybrid III's foam abdominal insert does not match the volume nor the loading response that is found in a human abdomen (Hardy et al., 2015). Furthermore, the abdomen of the Hybrid III does

not have any standard instrumentation, e.g., potentiometers, pressure sensors, etc., that could be used to evaluate abdominal injury risk. However, two abdominal inserts have been developed to improve the biofidelity and measurement capabilities of the Hybrid III abdomen. The Frangible Abdomen was made from crushable Styrofoam with protruding teeth to provide increased resistance to belt intrusion with increased abdominal compression, which resulted in a biofidelic force versus deflection response (Rouhana et al., 1989; 1990). The frangible design provided the ability to assess the occurrence of submarining, and the deformation was correlated to abdominal injury risk when submarining occurred. The Reusable Rate-Sensitive Abdomen (RRSA), which consisted of a fluid filled silicone shell, was designed to provide a biofidelic response in a variety of loading situations and had the capability to measure abdominal compression (Rouhana et al., 2001). However, the neither the Frangible Abdomen nor the RRSA are used in standard vehicle crash tests. More recently, the Test Device for Human Occupant Restraint (THOR) dummy has been developed to have a higher degree of abdominal biofidelity than the Hybrid III (Hardy et al., 2015). In addition, the THOR can measure lower chest deflection and abdominal deflection (Rangarajan et al., 1998). These deflection measurements could potentially be correlated to abdominal injury risk. However, there are currently no accepted abdominal risk functions based on these measurements. Despite improvements, ATDs are still not equipped to accurately predict individual abdominal organ injury risk. Therefore, it is necessary to perform simulations with finite element models to assess abdominal organ injury risk in MVCs. Although early FEMs modeled internal organs as a lump mass, more recent FEMs include individual internal organs (Lizee et al., 1998; Huang et al., 1994). The Global Human Body Modelling Consortium (GHBMC) abdomen contains all major soft

tissue organs and vessels (Gayzik et al., 2011). The Total Human Model of Safety (THUMS) model also includes individual internal organs (Kimpara et al., 2016). Although these more recent models incorporate individual thoracic and abdominal organs, they must be locally and globally validated using biomechanical data from material and structural testing in order to accurately predict the risk of injury to organs.

A number of studies have quantified the sub-failure and failure properties of liver at the tissue and whole organ level (Tables 1, 2, 3, and 4). These studies have shown that the material response of liver parenchyma, i.e., the functional tissue, is viscoelastic (Kemper et al., 2010; Kemper et al., 2013; Uehara, 1995; Pervin et al., 2011) and nonlinear (Kemper et al., 2010; Kemper et al., 2013; Pervin et al., 2011). In addition, liver parenchyma has been shown to respond differently in tension versus compression (Kemper et al., 2010; Kemper et al., 2013). Furthermore, bovine liver parenchyma has been shown to be isotropic, while porcine liver parenchyma has been shown to be transversely isotropic (Pervin et al., 2011; Chui et al., 2007). Material properties are also known to be different between the outer Glisson's capsule and the internal parenchyma tissue (Kemper et al., 2010).

A complication associated with soft tissue testing is that the response of biological tissue could potentially change significantly after death due to changes in temperature, hydration, blood supply, and postmortem degradation (Ottensmeyer, 2001). Since abdominal soft tissue degrades quickly after death, it is important to evaluate the effectiveness of preservation techniques in minimizing material and cellular changes between time of death

and testing. It has been shown that freezing bovine liver tissue significantly changes the material response, making it an unacceptable storage/preservation method (Santago et al., 2009b). Therefore, the tissue must be stored at an above freezing temperature and kept hydrated with an appropriate preservation fluid. Saline has been a commonly used preservation/hydration fluid in biomechanical studies performed on liver tissue (Popovic and Simic, 1989; Hollenstein et al., 2006; Tay et al., 2006; Sparks et al., 2007). However, the cellular architecture of liver tissue has been shown to change with increased postmortem time when the tissue is stored in saline (Popovic and Simic, 1989). Popovic and Simic (1989) observed cell swelling in guinea pig livers within a few hours postmortem when the tissue was stored in saline. Furthermore, sub-failure tests have quantified postmortem changes in the biomechanical response of the liver when stored in saline. A previous study conducted ramp-and-hold and indentation tests on porcine liver tissue at multiple time points up to 48 hours postmortem (Tay et. al., 2006). Tests were completed *in vivo*, *ex vivo*, and *in vitro*. The *in vitro* tissue was kept cool and stored in saline until testing at approximately 6, 24 and 48 hours postmortem. The results showed an increase in the stiffness of the liver with increased postmortem time. However, indentation tests only observe compressive behavior in the toe and linear regions of the stress-strain curve. Therefore, this study did not evaluate the failure properties of the tissue, which are essential for establishing tolerance levels in FEMs. Studies reporting failure properties of isolated animal liver parenchyma coupons have been limited to testing at 24 hours postmortem, or later (Tables 2 and 3). While failure studies conducted on isolated human parenchyma liver samples have been limited to testing within 48 hours postmortem. To the author's knowledge, no studies have evaluated the effects of postmortem time on liver parenchyma

failure properties within 24 hours of death. While changes in tissue failure response have not been fully quantified, the results from the above studies raise concern when considering the large duration of postmortem time that typically passes before biomechanical tests can be conducted.

In several recent studies Dulbecco's Modified Eagles Medium (DMEM) was used as the preservation fluid instead of saline (Santago et al., 2009a; Santago et al., 2009b; Kemper et al., 2010; Kemper et al., 2013; Lu et al., 2014). DMEM is a cell culture medium commonly used in studies involving hepatocyte cultures (Na et al., 2014; Jones et al., 2009; Mitaka et al., 1992). DMEM is composed of inorganic salts, amino acids, vitamins, and glucose. In a preliminary histological study, Kemper et al. (2013) investigated the effectiveness of DMEM in preserving liver cellular structure. In this study, a control tissue sample was taken from bovine livers at 24 hours postmortem while other samples were stored in DMEM for an additional 24 hour period. At the end of the 24 hour storage period, i.e., 48 hours postmortem, the cellular architectures were compared between the control sample and the stored samples. It was found that DMEM maintained the specimen hydration, preserved the cellular architecture of the parenchyma, and allowed only mild cell swelling. Since previous studies found changes in cellular architecture when liver tissue was stored in saline, but preserved cellular architecture when stored in DMEM, there is reason to hypothesize that DMEM may also preserve the failure properties more effectively. However, this assumption needs to be evaluated through a controlled biomechanical study.

The current study seeks to quantify the effects of postmortem degradation on the tensile failure material properties of liver parenchyma while stored in saline or DMEM, by conducting uniaxial tension tests at three time points postmortem (6hrs, 24hrs, and 48hrs). Furthermore, the current study investigates the relationship between changes in cellular architecture and changes in failure response. Finally, preliminary data are provided to investigate the effect of tissue storage block size during storage on the effects of postmortem degradation.

Table 1**:** Previous studies observing the effects of postmortem time on liver cellular structure.

	Cellular Level					
	Paper	**Liver Type**	**Test Type**	**Storage**	**Sample Time Postmortem (hrs)**	**Major Findings**
Histology Studies	Popovic and Simic (1989)	Guinea pig	Histology	Fresh, *In situ*, Saline	0,1,2,4 hr	Cell swelling and occasional disruptions of membranes within a few hours postmortem. Decreased cellular integrity with increased postmortem time.
	Kemper et al. (2013) (preliminary)	Bovine	Histology	Fresh, DMEM	~48 hr (Tissue stored for 24hr period)	DMEM maintained specimen hydration, preserved cellular architecture. Mild cell swelling.
	Tomita et al. (2004)	Rat	Histology	Fresh, *In Situ* at 23°C	1,3,5,10,15,24 hr	Cell edema was seen at one hour from death. Increase in mitochondrial cristae loss with postmortem time.

Table 2: Previous tensile biomechanical studies conducted on isolated liver tissue samples.

	Isolated Tissue Samples					
	Paper	**Liver Type**	**Test Type**	**Storage**	**Test Time Postmortem**	**Major Findings**
Tensile Material Property Testing	Santago et al. (2009a)	Bovine	Tensile (failure)	Fresh, DMEM	~24 hr	Testing temperature did not significantly affect failure stress and strain when between 75°F and 98°F.
	Santago et al. (2009b)	Bovine	Tensile (failure)	Fresh and Frozen, DMEM	24 hr, 26 days	Freezing bovine liver tissue significantly decreases failure strain.
	Kemper et al. (2010)	Human	Tensile (failure)	Fresh, DMEM	48 hr	Increase in loading rate results in increase in failure stress and decrease in failure strain.
	Uehara (1995)	Porcine	Tensile	Ringer's	?	The parenchyma tensile stress strength, extension ratio, and modulus change with respect to loading rate.
	Brunon et al. (2010)	Porcine, Human	Tensile (failure)	Fresh and Frozen, Fluid not reported	Unclear "fresh" 4 or 5 days +	Freezing significantly changed the material properties of porcine *capsule*.
	Lu et al. (2014)	Bovine	Tensile (failure)	Fresh and Frozen, DMEM	Fresh (~24 hr), 30 days, 60 days	Failure strain decreased significantly between fresh and previously frozen specimens. Increase in stiffness with increased preservation time and loading rate.
	Hollenstein et al. (2006)	Bovine	Tensile (failure), Aspiration	Fresh, Saline	8 hr	Determined nominal stress and strain data for 5 liver capsule samples. The number of tests were not sufficient for a statistical analysis. Results showed bilinear stress-stretch response for capsule samples.
	Gao et al. (2010)	Porcine	Pure Shear, Unconfined Compression, Uniaxial Tension	Frozen, water mist while thawing	Not reported	Proposed two new constitutive models to describe the non-linear stress-strain relation.
	Chui et al. (2007)	Porcine	Tensile, Compression, Combined	Frozen, Ringer's	24 hr	Porcine liver tissue is transversely isotropic.
	Stingl et al. 2002	Human	Tensile (failure)	Fresh *No fluid specified	>24-36hr *Not specified	Testing on liver *capsule*, not parenchyma. Capsule critical tension ranged from 0.066-0.386MPa. Additional results were not sufficient for statistical analysis.

Table 3: Previous compressive biomechanical studies conducted on isolated liver tissue samples.

	Isolated Tissue Samples					
	Paper	**Liver Type**	**Test Type**	**Storage**	**Test Time Postmortem**	**Major Findings**
Compressive Material Property Testing	Kemper et al. (2013)	Human	Compression (failure)	Fresh, DMEM	48 hr	Response of parenchyma is nonlinear and dependent on loading rate. Significant increase in failure stress and decrease in failure strain with increased loading rate.
	Pervin et al. (2011)	Bovine	Kolsky Bar, Compression (subfailure)	Fresh, Kreb	3 hr	Uniaxial compressive response is non-linear and strain rate dependent. Responses obtained from specimens along and perpendicular to liver surface were consistent (isotropic).
	Ocal et al. (2010)	Bovine	Impact, ramp and hold (subfailure)	Fresh, Lactated Ringer's	1,2,4,8,12,24, 36,48 hr	The whole liver was flushed with LR. Samples were taken at each time point. Liver tissue becomes stiffer and more viscous with postmortem time.
	Lu & Untaroiu (2013)	Porcine	Indentation (subfailure)	Fresh, Cooled, Frozen, Saline	4 hr, 20 days	Porcine liver tissue stored in cooling showed an increase in stiffness. Freezing did not change the tissue stiffness.
	Gao et al. (2010)	Porcine	Pure Shear Test, Unconfined Compression, Uniaxial Tension	Frozen, water mist while thawing	Not reported	Proposed two new constitutive models to describe the non-linear stress-strain relation.
	Chui et al. (2007)	Porcine	Tensile, Compression, Combined	Frozen, Ringer's	24 hr	Porcine liver tissue is transversely isotropic.

Table 4: Previous whole organ biomechanical studies.

	Whole Organ					
	Paper	**Liver Type**	**Test Type**	**Storage**	**Test Time Postmortem**	**Major Findings**
Whole Liver Tests	Brown et al. (2003)	Porcine, Bovine	Cyclic and step compression (subfailure)	Porcine: fresh, assumed unfrozen Bovine: previously frozen *No fluid specified	In Vivo In Situ: 3hr	Some difference found in stress relaxation behavior between successive conditions and between *in-vivo* and *in-situ*. Non-linear stress-strain behavior.
	Kerdok et al. (2006)	Porcine	Indentation (subfailure)	Fresh, Lactated Ringer's	In Vivo, Ex Vivo, In Vitro, average of 5 to 8 hr	Un-perfused conditions showed differences from *in vivo* condition. Specifically, un-perfused tissue had a stiffer and more viscous response. The *ex vivo* perfusion condition resulted in a response comparable to the *in vivo* response.
	Tay et al. (2006)	Porcine	Ramp and hold, indentation (subfailure)	Fresh, Saline	In Vivo, Ex Vivo, In Vitro: 6, 24, and 48 hr	Increase in stiffness with postmortem time.
	Sparks et al. (2007)	Human	Drop tower	Unspecified if fresh or previously frozen, Saline	36 hr	The product of the peak rate of tissue pressure increase and peak tissue pressure, and tissue pressure are both strong correlates to injury.
	Kemper et al. (2011)	Human	Indentation (subfailure) *failure tests conducted but not presented	Fresh, DMEM	48 hr	The whole organ response was non-linear and dependent on loading rate.

METHODS

Tension Testing

Uniaxial tension tests were conducted on isolated samples of fourteen bovine livers at three time points after death; 6, 24, and 48hrs (Figure 1). Tissue was stored in one of two different preservation fluids (DMEM or saline), and in one of three different storage sizes (large block, small block, or slice), as shown in Table 5. Each liver was obtained from a local slaughterhouse immediately after death. Approximately 45 minutes passed between the animal's time of death and when the liver was available. During transport to the lab (~50 minutes), livers were sealed in a plastic bag and placed on wet ice in a cooler. The livers were not frozen at any point during transport, testing, or storage, since freezing has been shown to affect the material properties of liver tissue (Santago et al., 2009b). Upon arrival at the lab, a portion of each liver was used immediately for fresh specimen preparation and testing, i.e. 6 hour time point. The remaining liver tissue that was not used for the 6 hour time point was stored in the assigned preservation fluid until testing at one of the latter two time points, i.e. 24 and 48 hours. The stored tissue was divided into sections and placed into containers. The containers were filled with the assigned preservation fluid so that the tissue was completely submerged, sealed, and kept cool by means of refrigeration until the 24 hour or 48 hour time points. The dimensions of "large" storage blocks were approximately 12cm x 8cm x 4cm. "Small" storage blocks were approximately 6cm x 3cm x 4cm. Tissue stored as slices were approximately 6cm x 0.5cm x 3.5cm.

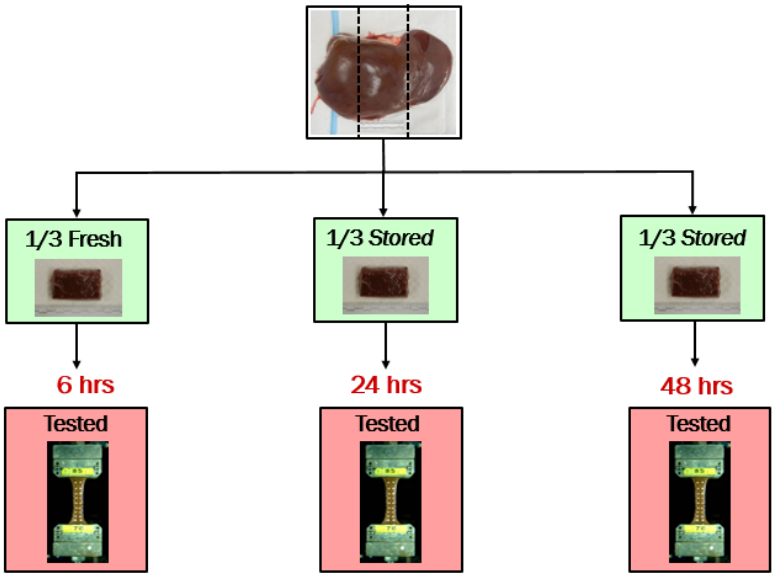

Figure 1: Timeline of liver procurement, storage, and preparation.

Table 5: Liver breed, tissue storage size, and preservation fluid assignments.

Liver	Breed	Tissue Storage Size	Preservation Fluid	Number of Successful Tests
D1	Angus	Large Blocks	DMEM	9
D2	Angus	Large Blocks	DMEM	9
D3	Angus	Large Blocks	DMEM	7
D4	Angus	Large Blocks	DMEM	9
D5*	Angus	Large Blocks	DMEM	9
D6	Angus	Large Blocks	DMEM	7
S1	Angus	Large Blocks	Saline	9
S2	Angus	Large Blocks	Saline	13
S3	Angus	Large Blocks	Saline	9
S4	White Park	Large Blocks	Saline	7
S5	Angus	Large Blocks	Saline	11
S6	Angus	Large Blocks	Saline	13
L1	White Park	Small Blocks & Slices	Saline	18
L2	Angus	Small Blocks & Slices	DMEM	18

*Note: Liver D5 was classified as cirrhotic by the slaughterhouse inspector.

A detailed procedure was followed to obtain multiple dog-bone samples from each liver (Kemper et al., 2010). The first step in obtaining dog-bone samples was to cut a rectangular block of tissue from the liver (Figure 2). The block was then placed into a custom slicing jig to secure the tissue during slicing. Long blades were inserted into guide slots and drawn horizontally across the block. The blades cut the tissue while exerting minimal downward force, resulting in tissue slices with constant thickness. The tissue slices were then stored in the assigned preservation fluid until stamping to maintain sample hydration. During stamping, each slice was laid on a stamping base between two guide rods. A template was placed over the sample using the guide rods to aid in positioning the tissue so that the final sample would not include visible vasculature or defects. After removing the template, a custom stamp was placed over the slice and struck firmly with a hammer to cut the tissue. The resulting dog-bone sample was then submerged in the assigned preservation fluid to maintain hydration until testing. The cutting and stamping process required approximately two hours to complete. Therefore, the cutting and stamping procedures began before the 6 hour, 24 hour, and 48 hour marks so that testing began around the 6 hour, 24 hour, and 48 hour marks.

In order to assess the effect of preservation time and fluid type on the cellular architecture, tissue samples were taken at each time point for histological analysis. Histology samples obtained from stored tissue were taken from a location near the center of the storage block or slice, away from the edges. Histology samples were stained with Hematoxylin and Eosin (H&E), and Masson's Trichrome, then analyzed by a certified veterinary pathologist. The veterinary pathologist graded each sample

based on the level of cellular disruption, i.e., swelling, dissociation, and nuclear dissolution, revealed by the H&E stain. A disruption score of 0 indicated normal cellular structure. A rating of 1 indicated mild cell swelling, while a rating of 2 indicated moderate cell swelling and dissociation. A rating of 3 indicated moderate cell swelling with dissociation and nuclear dissolution. The pathologist also graded each sample based on the level of fibrosis revealed primarily by the Masson's Trichrome stain. A fibrosis score of 0 indicated a normal level of fibrosis. A rating of 1 indicated mild periportal, while a rating of 2 indicated moderate periportal. A rating of 3 indicated moderate bridging. It was not expected that the level of fibrosis in a liver would change with time. However, variations in the level of fibrosis between livers could potentially explain variations in the material properties between livers.

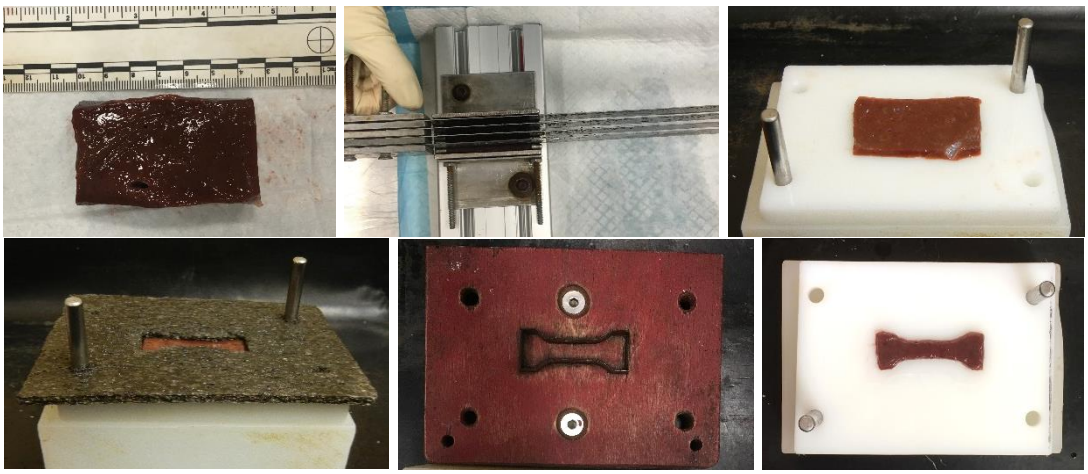

Figure 2: Tissue block (top left), slicing jig and blade assembly (top center), tissue slice on stamping base (top right), template over slice (bottom left), custom stamp (bottom center), and cut dog-bone sample (bottom right).

Uniaxial tension tests were conducted on the isolated dog-bone samples at room temperature. The testing device consisted of two motor driven linear stages (Parker Daedal, MX80S, Irwin, PA). Each of the stages was instrumented with a single-axis load cell (Interface, WMC-5, Scottsdale, AZ), accelerometer (Endevco, 7264B-2000 G, Irvine, CA), and potentiometer (Firstmark Controls, Creedmoor, NC). A multi-axis controller (Parker, ACR9000, Irwin, PA) and motor driver (Parker, ViX, Irwin, PA) were used to operate the system. A testing procedure was developed to maintain consistency in initial specimen slack and alignment (Kemper et al., 2010). First, the top grip assembly was laid flat on a table top (Figure 3). The specimen was positioned on the top grip so that the long axis of the specimen aligned with the main axis of the grip and load cell. Once aligned, the top portion of the sample was clamped into the top grip. White circular enamel paint markers were applied to the front surface of the specimen. Then, the top grip assembly was reattached to the testing device. The sample was allowed to hang under its own weight before being clamped into the bottom grip, which allowed for a proportionally consistent tensile preload. The grip-to-grip distance was then measured to determine the appropriate velocity that the grips would be moved away from each other in order to obtain a strain rate of ~1strain/sec. A high resolution digital camera was used to take side view pictures of the mounted sample in order to obtain initial specimen thickness (Figure 4). High-speed video was recorded of the front-face of the specimen during each test (Vision Research, Phantom V9.1, Wayne, NJ). The pre-test frames were used to determine initial specimen width.

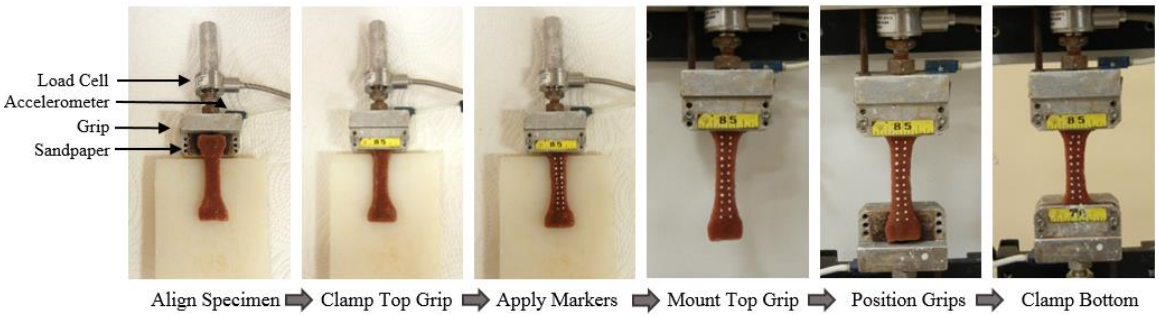

Figure 3: Procedure for mounting specimen onto test setup.

During the test, the top and bottom grips moved away from each other at a constant velocity applying tension to the specimen. Each specimen was loaded to failure at a strain rate of ~1strain/sec. The high-speed video was recorded at 500frames/sec with a resolution of 10.3pixels/mm. Load cell, potentiometer, and accelerometer data were sampled at 20,000Hz (Diversified Technical Systems, TDAS PRO, Seal Beach, CA).

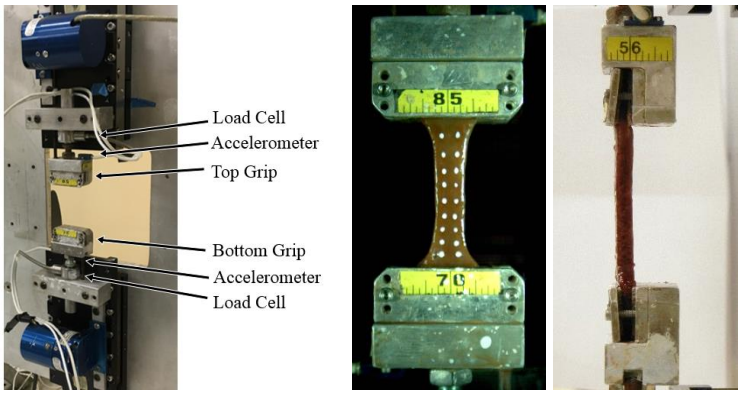

Figure 4: Uniaxial experimental setup (left) and mounted tissue specimen (center, right).

Data Processing

A test was considered successful if the failure tear occurred in the gage region of the dog-bone specimen. If a specimen tore next to the grip, or slipped out of the grip, then it was not included in the data set. For each successful test, the white optical markers were tracked using a motion analysis software (Image Systems, TEMA, Sweden). The distances between the markers surrounding the failure tear were used to calculate the stretch ratio (λ) and Green-Lagrangian Strain (E) (Equations 1 and 2). The instantaneous vertical distance between two dots (L_n) was determined at each video frame, while the original distance (L_o) was determined from a pre-movement frame. The vertical distance between the dots was best fit with a 6th degree polynomial from the time the grips began moving until the time of failure (Kemper et al., 2010). The average, minimum, and maximum R^2 values were 0.999, 0.994, and 1.000, respectively. Time of failure was defined as the visual initiation of the failure tear in the video.

$$\lambda = \frac{L_n}{L_o} \quad \text{(Equation 1)}$$

$$E = \frac{1}{2}(\lambda^2 - 1) \quad \text{(Equation 2)}$$

The grip acceleration (a), effective mass (m_{eff}), and measured force (F) were used to calculate the inertia compensated force (F_{IC}) and 2nd Piola Kirchhoff Stress (S) (Equations 3 and 4). The effective mass was defined as half the load cell mass in addition to the mass between the load cell and sample. The load cell and acceleration data were filtered to CFC 180 before inertial compensation. The inertia compensated force was fit using a 6th degree polynomial from the approximate time the grips began moving until the failure tear initiated. The average, minimum, and maximum R^2 values

were 0.999, 0.991, and 1.000, respectively. The stretch ratio, initial cross-sectional area at the tear location (A_o), and inertia compensated force were then used to calculate the 2nd Piola Kirchhoff Stress.

$$F_{IC} = F - a * m_{eff} \quad \text{(Equation 3)}$$

$$S = \frac{F_{IC}}{\lambda * A_o} \quad \text{(Equation 4)}$$

The modulus was quantified by applying a linear curve fit line to the linear region of each stress-strain curve. The linear region was defined as approximately 35% to 65% of the failure stress. The modulus was defined as the slope of the linear curve fit line. The average, minimum, and maximum R^2 values were 0.999, 0.995, and 1.000, respectively.

The modulus, failure stress, and failure strain were determined for each sample to allow for comparisons and statistical analyses. The values of each variable were averaged among the successful tests within each time point for each liver. Then, the average modulus and failure values were compared across the three time points for each liver and across all livers. The average modulus and failure values were also normalized for each liver by dividing the average value at each time point by the average value at the first time point. A Linear Mixed Effect Model with a random intercept effect and a fixed time effect was used to determine significant changes in the modulus, failure stress, or failure strain with respect to postmortem time. Significance was defined as $p \leq 0.05$.

RESULTS

Large Block Storage Samples:

A total of 243 tests were conducted from tissue stored as large blocks, resulting in 112 successful tests. Of the successful tests, 50 were from tissue stored in DMEM and 62 were from tissue stored in saline. For all livers stored as large blocks, there were between two and five successful tests per time point. The average testing times were 5.2±0.9hrs, 25.4±1.6hrs, and 48.8±1.8hrs at the 6hr, 24hr, and 48hr time points, respectively. The average failure stress across all six livers stored as large blocks in DMEM were 37.25±16.56kPa, 40.43±13.29kPa, and 36.24±12.49kPa at the 6hr, 24hr, and 48hr time points, respectively. The average failure strain were 0.234±0.050, 0.220±0.030, and 0.236±0.035, at the 6hr, 24hr, and 48hr time points, respectively (Table 6). The average failure stress across all six livers stored as large blocks in saline were 47.00±15.47kPa, 51.98±17.03kPa, and 50.52±22.88kPa at the 6hr, 24hr, and 48hr time points, respectively. The average failure strain were 0.268±0.034, 0.240±0.034, and 0.234±0.022, at the 6hr, 24hr, and 48hr time points, respectively (Table 7). Figures 5 and 6 compare the stress-strain curves from each liver specimen stored in large blocks at each time point. Figures 7 and 8 compare the average failure stress and strain for each liver across the three time points. Figures 9 and 10 compare the average failure stress and strain normalized to the 6hr time point failure values. The statistical analysis showed that the failure strain significantly decreased with respect to storage time for tissue stored as large blocks in saline (p-value = 0.009). The failure stress did not significantly change with respect to storage time for tissue stored in saline (p-value = 0.694). Neither the failure stress nor strain changed significantly

with respect to storage time for tissue stored as large blocks in DMEM (p-value = 0.782, 0.872).

Table 6: Average failure stress and strain values for each liver stored in DMEM.

Liver #	6hr		24hr		48hr	
	Failure Stress (kPa)	**Failure Strain** (strain)	**Failure Stress** (kPa)	**Failure Strain** (strain)	**Failure Stress** (kPa)	**Failure Strain** (strain)
D1	68.57	0.195	47.67	0.265	54.01	0.250
D2	39.41	0.219	49.00	0.207	28.56	0.258
D3	32.80	0.244	45.36	0.222	41.15	0.234
D4	26.64	0.210	17.76	0.172	21.67	0.183
D5	21.59	0.208	30.97	0.225	26.85	0.209
D6	34.48	0.330	51.83	0.231	45.21	0.281
Average	**37.25**	**0.234**	**40.43**	**0.220**	**36.24**	**0.236**
Std Dev	**16.56**	**0.050**	**13.29**	**0.030**	**12.49**	**0.035**

Table 7: Average failure stress and strain values for each liver stored in saline.

Liver #	6hr		24hr		48hr	
	Failure Stress (kPa)	**Failure Strain** (strain)	**Failure Stress** (kPa)	**Failure Strain** (strain)	**Failure Stress** (kPa)	**Failure Strain** (strain)
S1	62.69	0.292	57.25	0.287	95.01	0.237
S2	50.61	0.307	80.67	0.263	42.55	0.270
S3	26.03	0.285	33.25	0.220	35.28	0.235
S4	55.64	0.244	46.40	0.252	32.72	0.232
S5	57.61	0.266	56.41	0.224	51.80	0.230
S6	29.39	0.216	37.92	0.194	45.73	0.201
Average	**47.00**	**0.268**	**51.98**	**0.240**	**50.52**	**0.234**
Std Dev	**15.47**	**0.034**	**17.03**	**0.034**	**22.88**	**0.022**

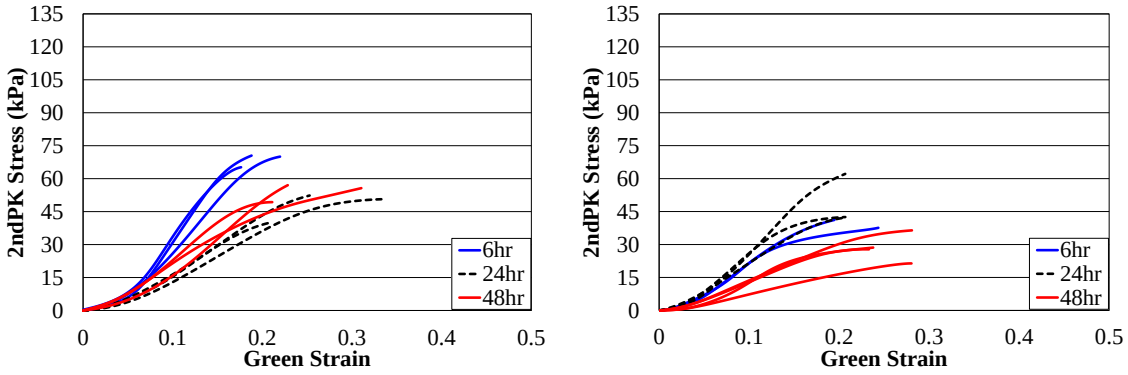

(a) D1 (b) D2

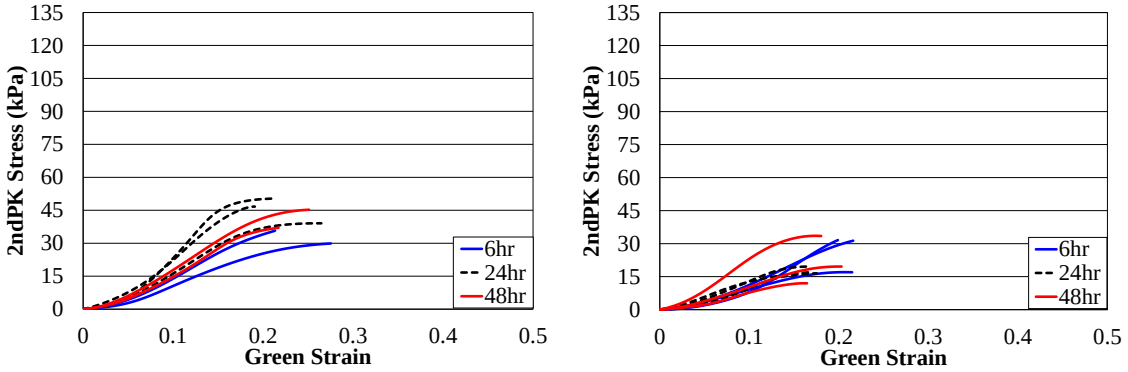

(c) D3 (d) D4

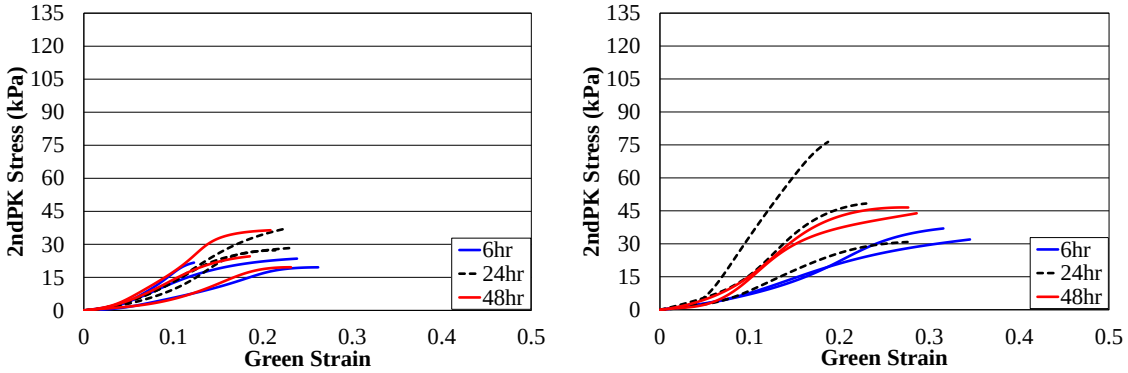

(e) D5 (f) D6

Figure 5: Stress-strain curves from all successful liver samples stored in DMEM.

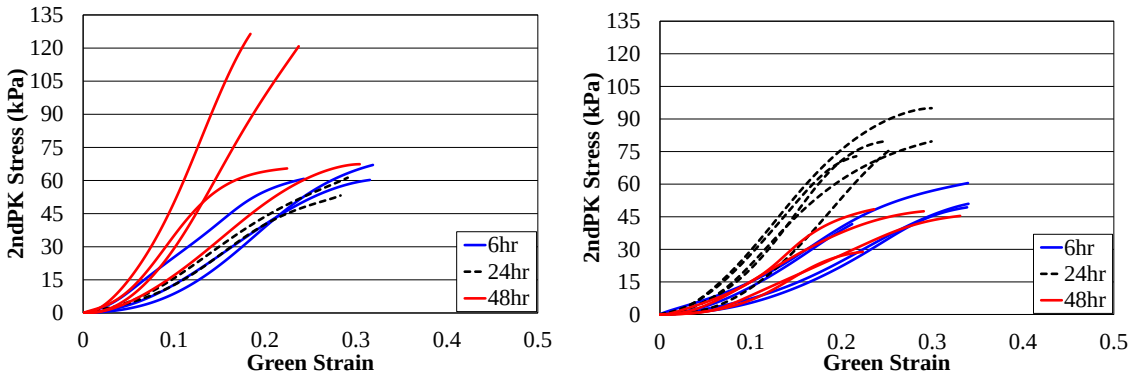

(a) S1 (b) S2

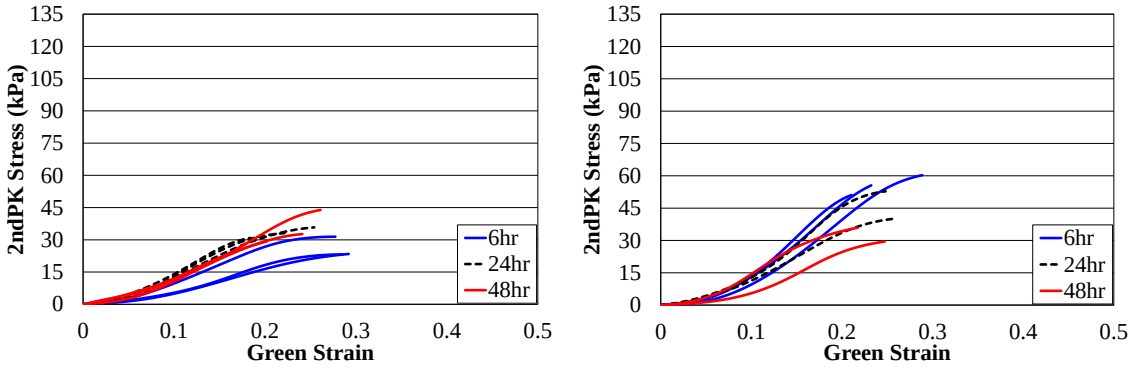

(c) S3 (d) S4

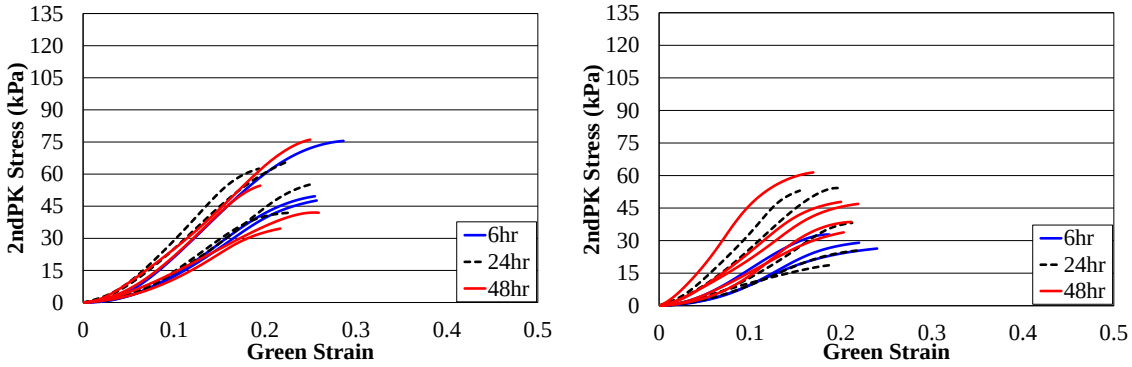

(e) S5 (f) S6

Figure 6: Stress-strain curves from all successful liver samples stored in saline.

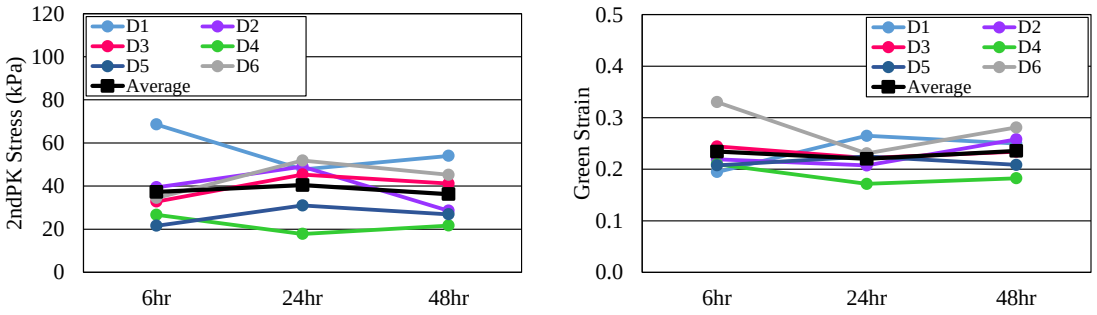

Figure 7: DMEM average failure stress (left) and strain (right) at each time point.

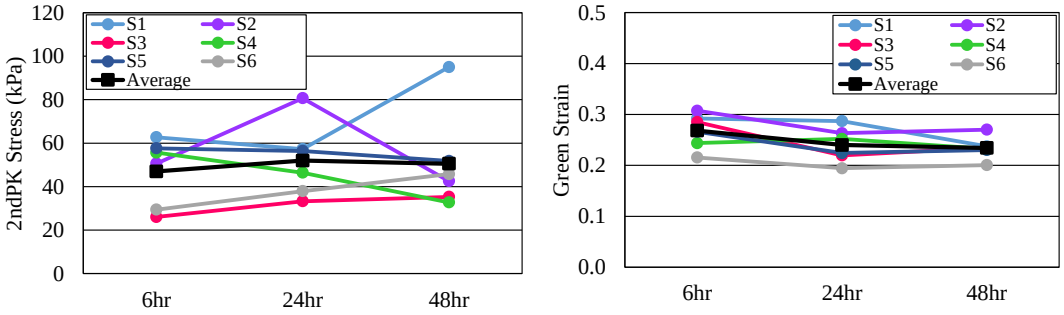

Figure 8: Saline average failure stress (left) and strain (right) at each time point.

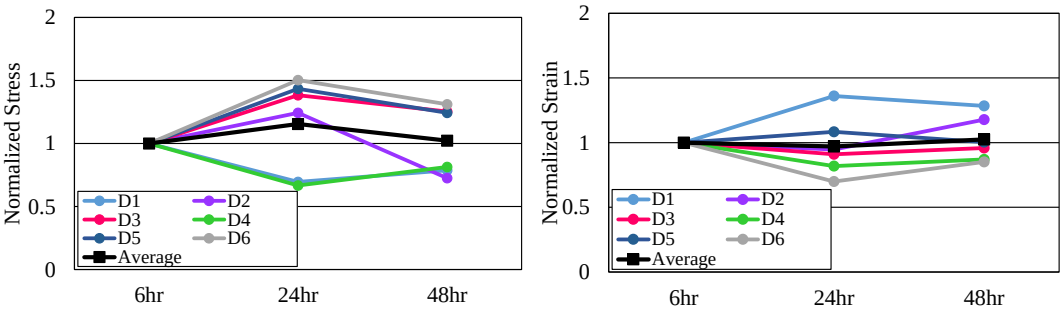

Figure 9: DMEM normalized average failure stress (left) and strain (right) at each time point.

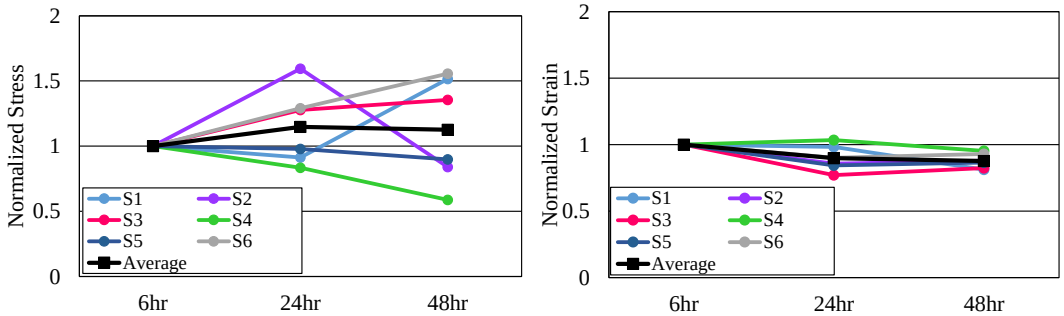

Figure 10: Saline normalized average failure stress (left) and strain (right) at each time point.

Modulus - Large Block

The average modulus was determined for each liver at each time point, as shown in Tables 8 and 9. The average modulus across all six livers stored as large blocks in DMEM were 269.0±155.7kPa, 292.1±87.2kPa, and 246.5±68.0kPa at the 6hr, 24hr, and 48hr time points, respectively. The average modulus across all six livers stored as large blocks in saline were 270.0±79.2kPa, 321.3±89.8kPa, and 335.9±158.8kPa at the 6hr, 24hr, and 48hr time points, respectively. Figure 11 compares the average modulus for each liver across the three time points. Figure 12 compares the average modulus normalized to the 6hr failure values. The statistical analysis showed that the modulus did not change significantly with respect to storage time for either DMEM or saline (p-value=0.666, 0.311).

Table 8: Average modulus for each liver stored in DMEM.

Liver #	**6hr**	**24hr**	**48hr**
	Modulus (kPa)	**Modulus** (kPa)	**Modulus** (kPa)
D1	565.2	263.3	318.0
D2	319.6	355.6	172.7
D3	201.0	353.4	256.3
D4	188.8	160.1	185.6
D5	179.7	234.8	212.6
D6	159.8	385.4	333.9
Average	**269.0**	**292.1**	**246.5**
Std Dev	**155.7**	**87.2**	**68.0**

Table 9: Average modulus for each liver stored in saline.

Liver #	6hr Modulus (kPa)	24hr Modulus (kPa)	48hr Modulus (kPa)
S1	315.2	292.5	642.9
S2	244.4	481.7	255.0
S3	145.7	228.0	208.5
S4	354.2	292.1	245.5
S5	334.8	362.5	310.8
S6	225.8	271.2	352.9
Average	**270.0**	**321.3**	**335.9**
Std Dev	**79.2**	**89.8**	**158.8**

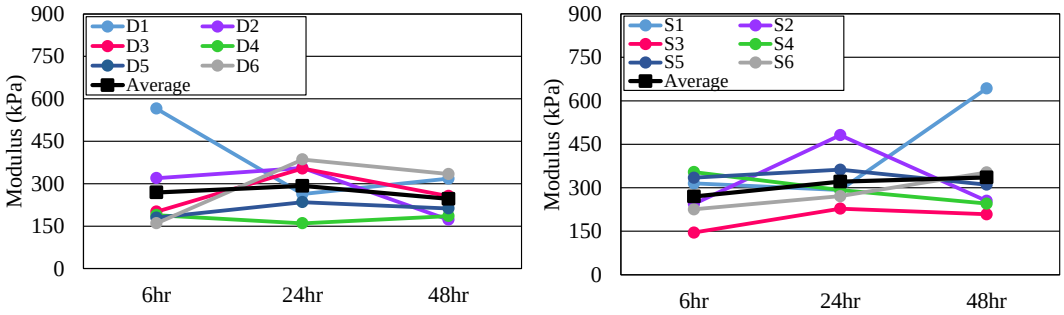

Figure 11: DMEM (left) and saline (right) average modulus at each time point.

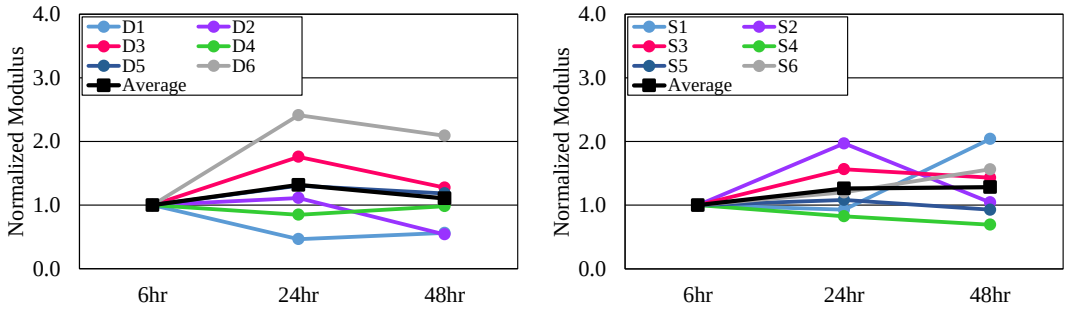

Figure 12: DMEM (left) and saline (right) normalized average modulus at each time point.

Histology - Large Block

Histology samples were graded based on cellular disruption and level of fibrosis. Example photos of histology samples are shown in Figure 13. Cellular disruption was graded on a scale of 0 to 3 for each time point, as shown in Table 10. Figures 14 and 15 show the increase in disruption relative to the 6hr score. The livers that showed the greatest increase in cellular disruption across the three time points were stored in saline (S1, S2, and S5). Livers D5 and S4 showed no increase in cellular disruption. It should be noted that liver S4 was a different breed, i.e., white park, than the other livers, i.e., angus, stored as large blocks. Figure 16 compares the average relative disruption scores from DMEM and saline livers, including and excluding the white park liver, S4. Figure 17 shows a decrease in normalized failure strain with an increase in relative cellular disruption grade. Figure 18 shows the same relationship between normalized strain and raw disruption scores without accounting for the time point. Fibrosis was graded on a scale of 0 to 3 for each time point. Table 11 shows that the fibrosis scores did not change with respect to time, which is to be expected. The two livers that showed the highest level of fibrosis were S4 and S5. All livers had a fibrosis rating of 0 or 1, indicating that the level of fibrosis should not interfere with analyses.

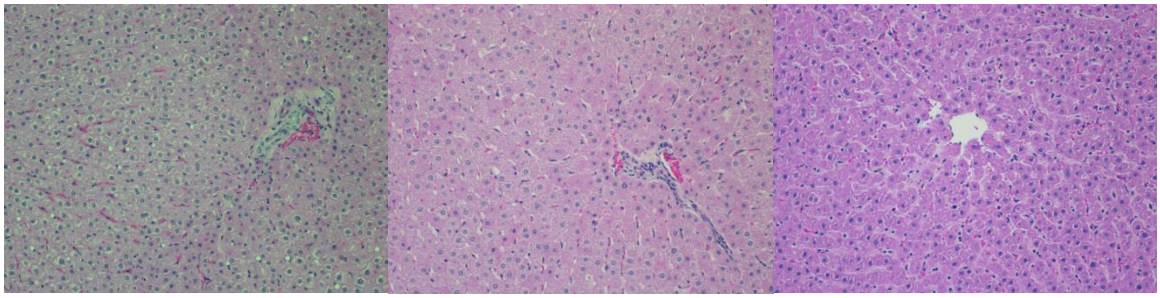

Figure 13. Examples of histology sections with the H&E stain and disruption scores of 0 (left), 1 (middle), and 2 (right).

Table 10: Cellular disruption histology ratings for tissue samples stored in DMEM and saline.

	Cellular Disruption Score		
Liver #	**6hr**	**24hr**	**48hr**
D5	0	0	0
D6	1	2	2
S1	0	1	2
S2	0	1	2
S3	0	1	1
S4	0	0	0
S5	0	1	2
S6	1	1	2

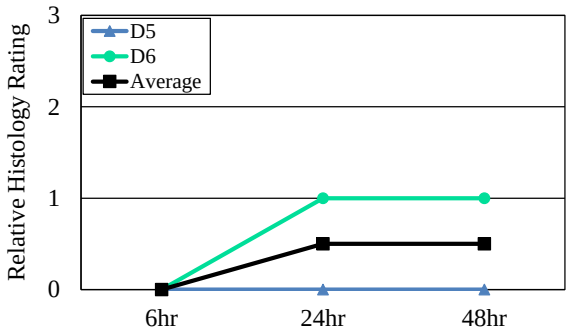

Figure 14: Cellular disruption scores relative to the 6hr time point for DMEM livers.

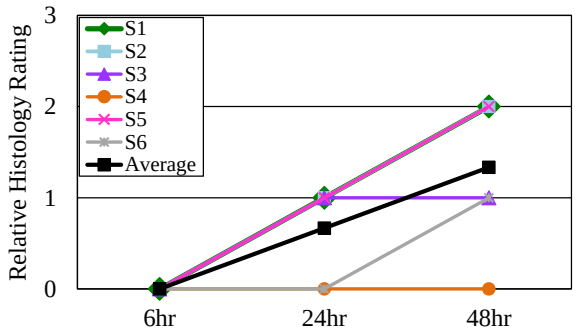

Figure 15: Cellular disruption scores relative to the 6hr time point for saline livers.

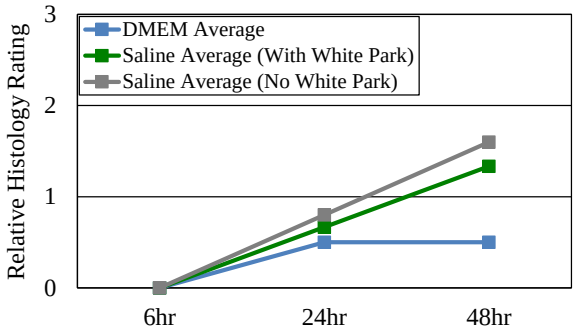

Figure 16: Relative cellular disruption score averages for DMEM and saline livers, with and without the white park liver.

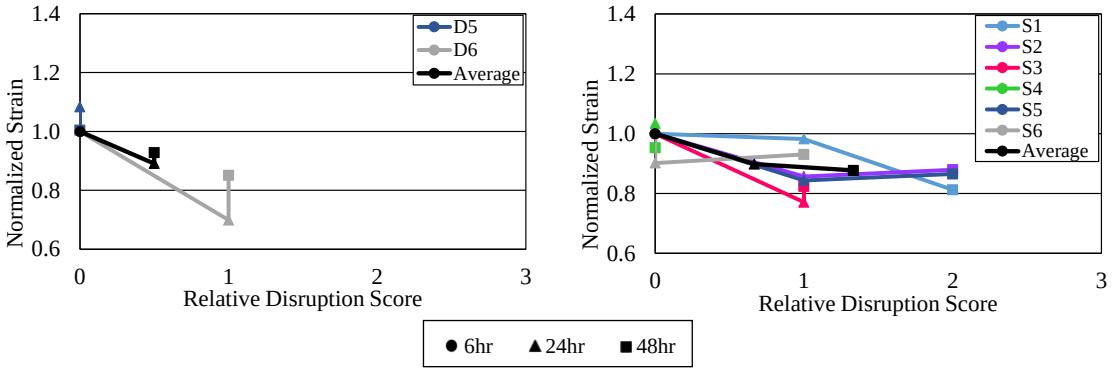

Figure 17: Normalized strain and relative disruption scores for DMEM (left) and saline livers (right).

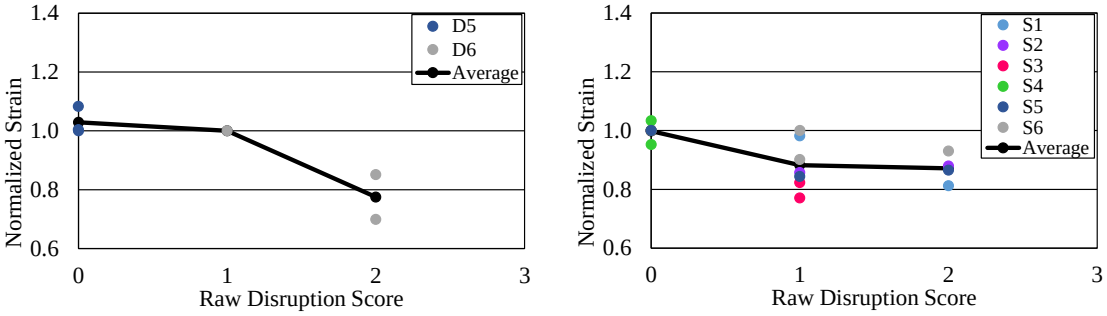

Figure 18: Normalized strain and raw disruption scores for DMEM (left) and saline livers (right). Note: Average calculated for each disruption grade, i.e., the plot does not show time progression.

Table 11: Fibrosis histology ratings for tissue samples stored in DMEM and saline.

	Fibrosis Score		
Liver #	**6hr**	**24hr**	**48hr**
D5	0	0	0
D6	0	0	0
S1	0	0	0
S2	0	0	0
S3	0	0	0
S4	1	1	1
S5	1	1	1
S6	0	0	0

Small Block and Slice Storage Samples:

A total of 71 tests were conducted from tissue stored as small blocks or slices, resulting in 36 successful tests. The failure stress and strain from the two livers stored as small blocks and slices are shown in Table 12. Figures 19 and 20 compare the stress-strain curves between the storage tissue sizes for each liver. Figures 21 and 22 compare the average failure stress and strain for each liver across the three time points. Figures 23 and 24 compare the average failure stress and strain normalized to the 6hr failure values. The failure strain decreased between the 6hr and 24hr time points, then plateaued or increased between the 24hr and 48hr time points, for tissue stored in saline and DMEM. The failure stress decreased between the 6hr and 24hr time points, then plateaued between 24hr and 48hr, for all tissues except those stored as small blocks in DMEM. No statistical analysis was conducted on the small block or slice data since only one liver was tested per fluid under this condition.

Table 12: Average failure stress and strain from tissue stored as small blocks or slices.

			6hr		**24hr**		**48hr**	
Liver #	**Fluid**	**Storage Size**	**Failure Stress** (kPa)	**Failure Strain** (strain)	**Failure Stress** (kPa)	**Failure Strain** (strain)	**Failure Stress** (kPa)	**Failure Strain** (strain)
L1 Size	Saline	Small block	64.92	0.274	44.19	0.193	50.99	0.212
		Slice	64.92	0.274	38.93	0.185	42.60	0.218
L2 Size	DMEM	Small block	115.24	0.225	83.41	0.175	34.13	0.197
		Slice	115.24	0.225	35.23	0.182	40.71	0.171

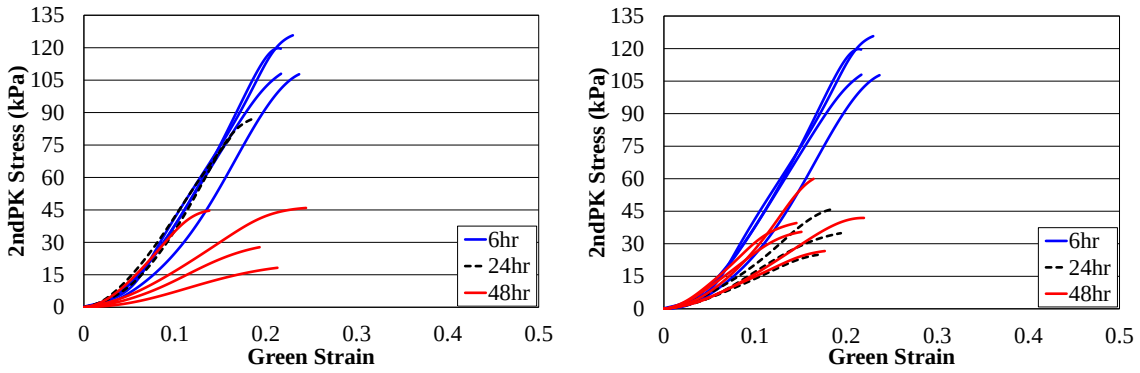

(a) L2 - Small Block (b) L2 - Slice

Figure 19: Stress-strain curves from the storage size variation liver stored in DMEM for the three time points.

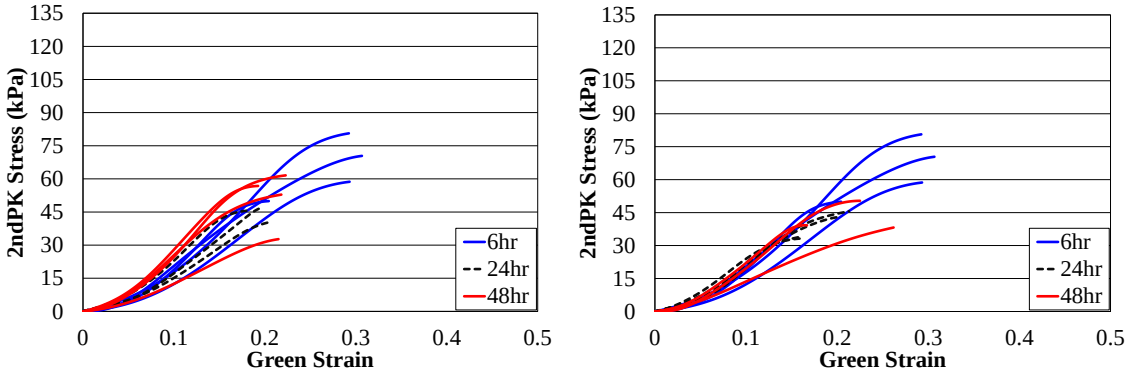

(a) L1 - Small Block (b) L1 - Slice

Figure 20: Stress-strain curves from the storage size variation liver stored in saline for the three time points.

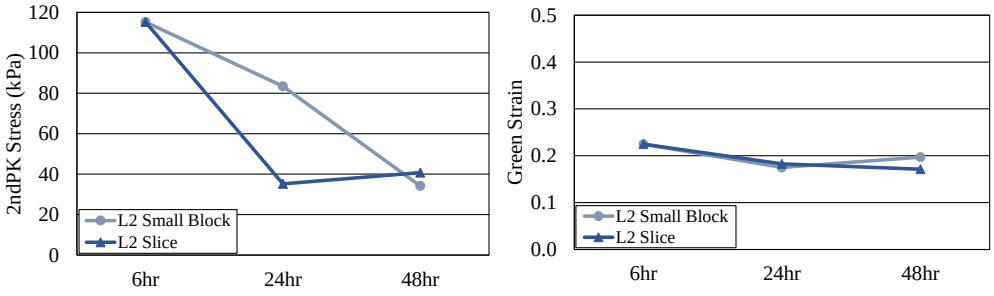

Figure 21: Average failure stress (left) and strain (right) from tissue stored as small blocks and slices in DMEM.

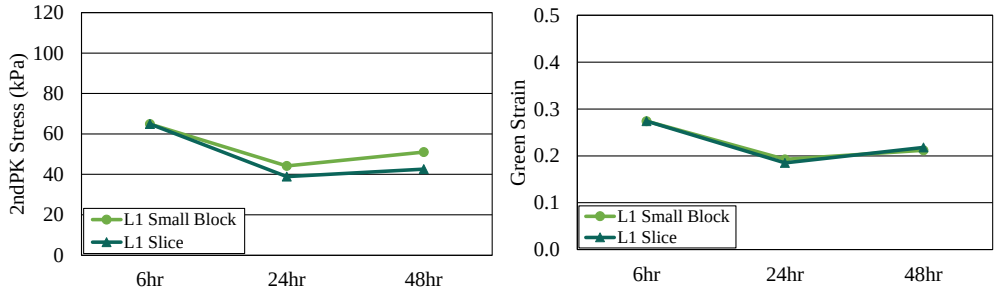

Figure 22: Average failure stress (left) and strain (right) from tissue stored as small blocks and slices in saline.

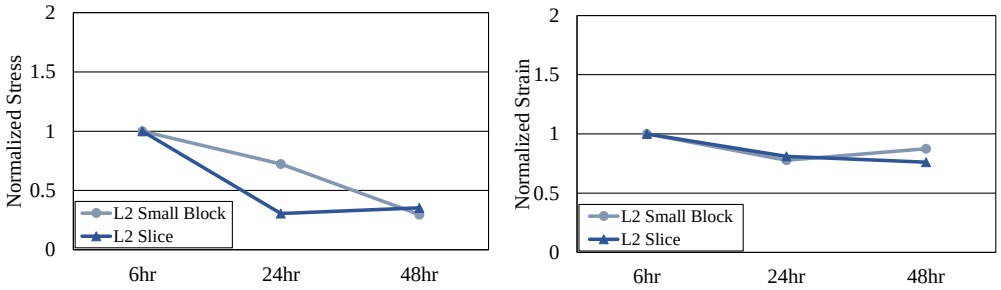

Figure 23: Normalized average failure stress (left) and strain (right) from tissue stored as small blocks and slices in DMEM.

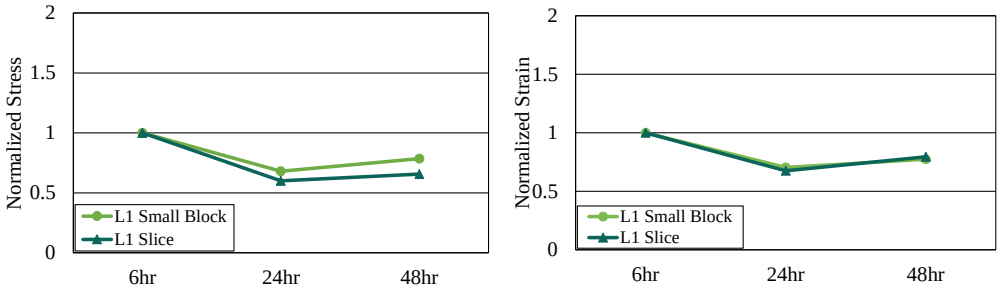

Figure 24: Normalized average failure stress (left) and strain (right) from tissue stored as small blocks and slices in saline.

Modulus - Small Block and Slice

Table 13 and Figure 25 show the average modulus at each time point determined for the livers stored as small blocks and slices. Figure 26 compares the average modulus normalized to the 6hr modulus value. The average modulus did not noticeably change with respect to postmortem time for tissue stored in saline. Conversely, there was a clear decrease in average modulus for tissue stored in DMEM. No statistical analysis was conducted since only one liver was tested per fluid under this condition.

Table 13: Average modulus from tissue stored as small blocks and slices.

			6hr	**24hr**	**48hr**
Liver #	**Fluid**	**Storage Size**	**Modulus** (kPa)	**Modulus** (kPa)	**Modulus** (kPa)
L1 Size	Saline	Small block	363.5	319.6	374.1
		Slice	363.5	345.5	284.0
L2 Size	DMEM	Small block	700.9	667.2	266.4
		Slice	700.9	260.6	335.4

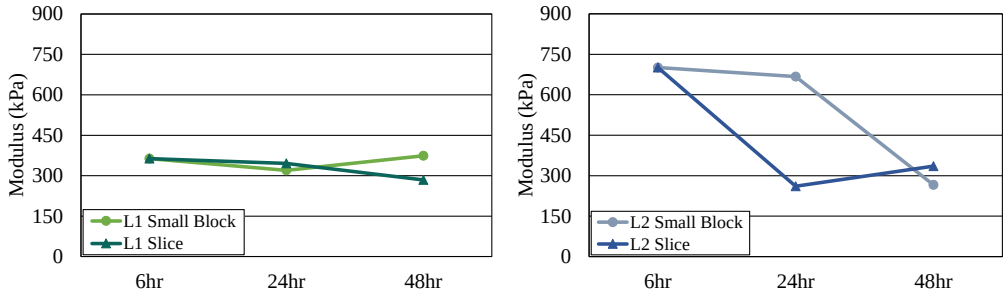

Figure 25: Average modulus from tissue stored as small blocks and slices in saline (left) and DMEM (right).

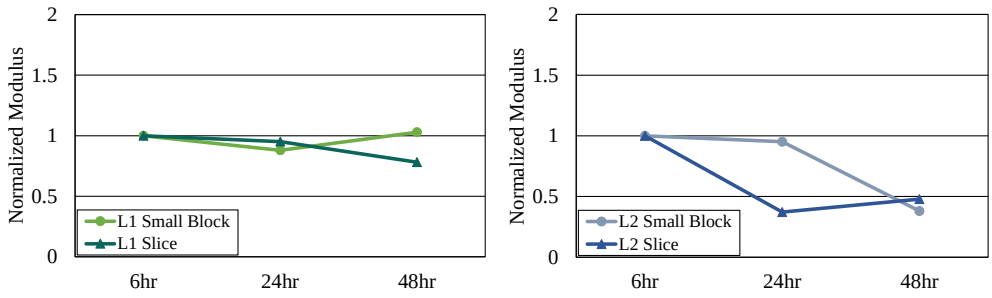

Figure 26: Normalized average modulus from tissue stored as small blocks and slices in saline (left) and DMEM (right).

Histology - Small Block and Slice

Of the two livers stored as small blocks and slices, the tissue stored in saline showed more cellular disruption for a given specimen storage size (Table 14). Figure 27 shows an increase in relative disruption across the three time points. Figure 28 shows a decrease in normalized strain with increased relative disruption across the time points. Figure 29 shows the same relationship between normalized strain and raw disruption scores without accounting for the time point. Both livers had a fibrosis score of 0 or 1 that did not change across time points, as shown in Table 15.

Table 14: Cellular disruption histology ratings for tissue samples stored as small blocks or slices in saline and DMEM.

		Cellular Disruption Score		
Liver #	**Fluid**	**6hr**	**24hr**	**48hr**
L1-Small Block	Saline	0	1	2
L1-Slice		0	2	3
L2-Small Block	DMEM	0	0	1
L2-Slice		0	1	2

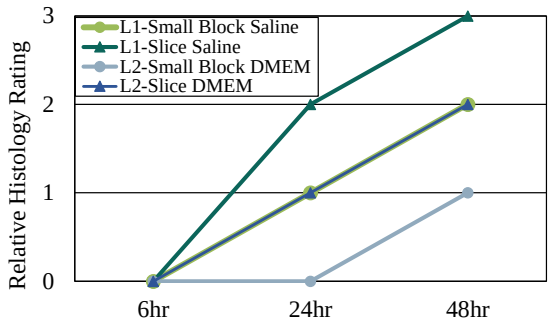

Figure 27: Cellular disruption for tissue stored as small blocks and slices in saline and DMEM.

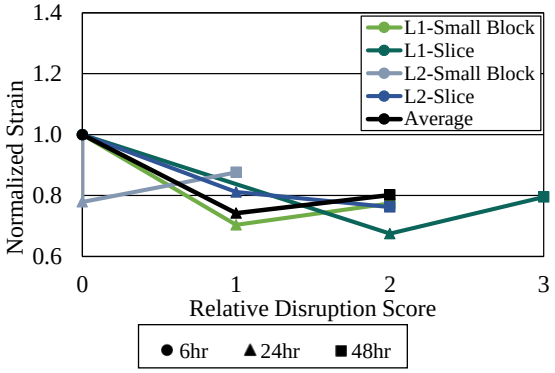

Figure 28: Normalized strain and relative disruption scores for tissue stored as small blocks and slices for each time point.

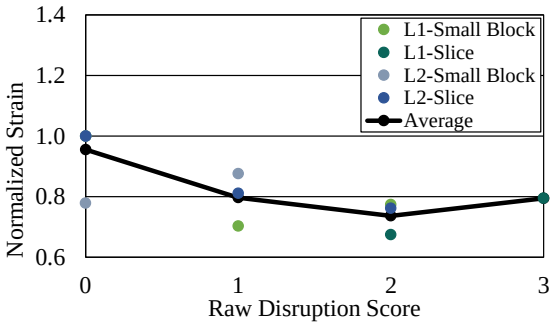

Figure 29: Relationship between normalized strain and raw disruption scores for tissue stored as small blocks and slices.

Table 15: Fibrosis histology ratings for tissue samples stored as small blocks or slices in saline and DMEM.

		Fibrosis Score		
Liver #	**Fluid**	**6hr**	**24hr**	**48hr**
L1-Small Block	Saline	1	1	1
L1-Slice		1	1	1
L2-Small Block	DMEM	0	0	0
L2-Slice		0	0	0

Large Block, Small Block, and Slice Storage Samples Combined:

Figure 30 shows a decrease in normalized strain with the increase in relative disruption across the time points for all livers included in this study. Figure 31 shows the same relationship between normalized strain and raw disruption scores without accounting for the time point.

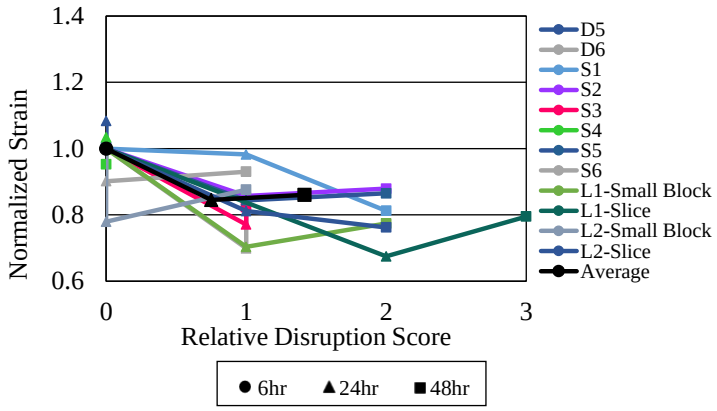

Figure 30: Normalized strain and relative disruption scores for all livers included in this study for each time point.

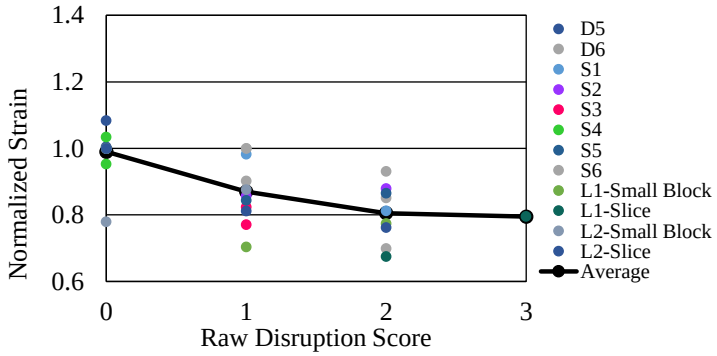

Figure 31: Relationship between normalized strain and raw disruption scores for all livers included in this study.

DISCUSSION

To the author's knowledge, the current study is the first to quantify the tensile failure properties of liver parenchyma less than 24 hours postmortem. However, previous studies have reported failure properties of bovine or human liver parenchyma at 24 hours or 48 hours postmortem. The tensile failure stress and strain from the current study are generally consistent with those reported in previous studies (Figure 32). Lu et al. (2014) conducted uniaxial tensile tests on samples from ten fresh bovine livers approximately 24 hours postmortem. The 2nd Piola Kirchhoff failure stress and Green-Lagrangian failure strain were calculated from tests conducted at one of three strain rates, including ~1s^{-1}. The average local failure values were not explicitly reported. However, it was determined that the failure stress was approximately 56kPa±25Pa, and the average failure strain was approximately 0.29±0.08. The average maximum stress and strain reported by Santago et al. (2009a) for all samples from two fresh bovine livers tested at approximately 24 hours postmortem at room temperature were 54.79±25.68kPa and 0.25±0.06. In the current study, the average failure stress and strain at 24 hours postmortem were 40.43±13.29kPa and 0.22±0.03 for tissue stored in DMEM, and 51.98±17.03kPa and 0.24±0.03 for tissue stored as large blocks in saline. However, the values from Santago et al. (2009a) are not a direct comparison to the current study because they were tested at a lower strain rate of 0.07s^{-1}. Kemper et al. (2010) reported average failure stress and strain values of 52.61±25.73kPa and 0.30±0.10 from human liver parenchyma tested at a strain rate of ~1s^{-1} within 48 hours from death. The average failure stress and strain at 48 hours postmortem in the current study were 36.24±12.49kPa and 0.24±0.04 for tissue stored in DMEM, and 50.52±22.88kPa and 0.23±0.02 for tissue stored as large blocks in saline.

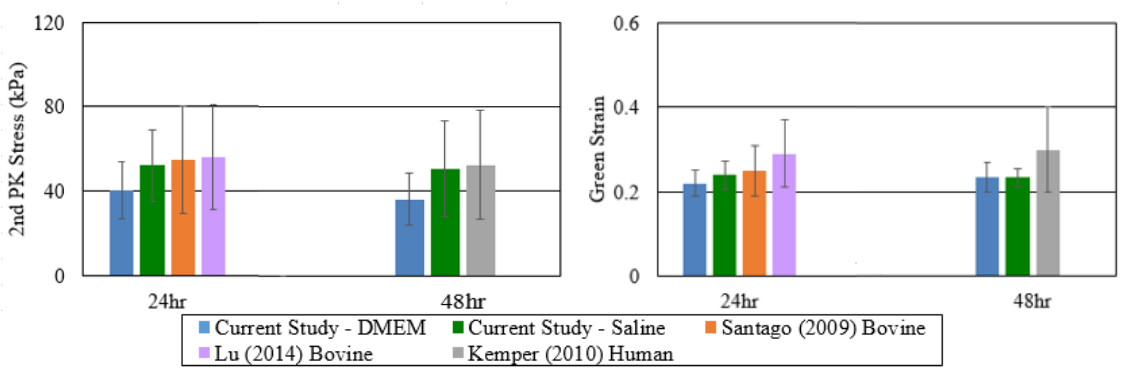

Figure 32: Comparison of failure stress (left) and strain (right) reported in previous studies.

The modulus values from the current study can also be compared to those reported in previous studies. Yeh et al. (2002) measured the elastic modulus of human liver samples using a cyclic compression-relaxation method within 48 hours of removal from the body. In this study, the modulus was calculated from the engineering stress-strain curve and correlated with a fibrosis histology score. The score ranged from '0' (no fibrosis) to '4' and '5' (cirrhosis). A fibrosis score of '1' signified portal fibrosis without septa. The strain was defined as the ratio of the change in height to the initial height. The average elastic moduli for samples with a fibrosis score of '0' were 0.64±.08kPa (5% preload strain) and 2.00±0.63kPa (15% preload strain). One specimen with a fibrosis score of '1' resulted in moduli of 1.26kPa (5% preload strain) and 6.80kPa (15% preload strain). In order to compare the moduli from the current study to the human data from Yeh et al. (2002), the stress and strain data from the current study were converted to engineering stress and strain. The subsequent average modulus calculated in the current study was 345.1±155.4kPa and 427.0±184.7kPa, for large block tissue stored in DMEM and saline, respectively. The difference in the average modulus between these two studies is likely due to the fact that the human livers used by Yeh et al. (2002) were subjected to cyclic, sub-failure,

compression-relaxation loading, rather than tensile failure loading. When comparing the sub-failure stress and strain values reported by Yeh et al. (2002) to the stress-strain curves from the compressive failure tests reported by Kemper et al. (2013), it is clear that the modulus values reported by Yeh et al. (2002) are from the toe region of the stress-strain curve. Uehara (1995) conducted tension tests on porcine liver parenchyma samples at various strain rates. The average moduli reported at strain rates from 5mm/min to 500mm/min ranged from 684±70kPa to 1,190±124kPa, respectively. In order to compare the data from the current study to the data reported by Uehara (1995), the stress and strain data from the current study were converted to true stress and true strain, by assuming a Poisson's ratio of 0.5. The average modulus from the true stress versus true strain curves was then calculated to be 445.1±197.3kPa and 570.7±242.5kPa for tissue stored as large blocks in DMEM and saline, respectively. It is reasonable that the modulus of bovine liver parenchyma was found to be lower than that of porcine liver parenchyma given that Kemper et al. (2010) reported that porcine parenchyma has a higher failure stress but similar failure strain compared to human or bovine. Furthermore, Stingl et al. (2002) conducted tension tests on human liver capsule specimens with sub-capsule tissue attached. The reported modulus of elasticity ranged from 315.5kPa to 2,850.3kPa. Neither the loading rate nor the method of calculating stress and strain were reported. However, it was expected that the capsule of the liver would be stiffer than the underlying parenchyma given that the liver capsule is comprised primarily of collagen.

The current study is the first to quantify the changes in tensile failure material properties and modulus between 6 and 48 hours postmortem. The failure strain decreased significantly

with respect to postmortem time for tissue stored as large blocks in saline. Similarly, previous studies have reported a change in the sub-failure response of liver tissue with increased storage time when the tissue was stored in saline. Tay et al. (2006) measured reaction forces using an indentation stimulus to probe whole porcine livers while *in vivo*, *ex vivo*, and *in vitro*. *In vitro* tissue was kept cool in a saline bath for 6 to 48 hours postmortem for testing at multiple time points. The liver response showed an increase in stiffness with an increase in postmortem time. Ocal et al. (2010) found similar results while investigating the effect of preservation period on the dynamic material properties of bovine liver tissue. In this study, the livers were flushed with and stored in lactated ringer's solution, and kept cool. Cylindrical samples were extracted at multiple time points between 1 and 48 hours postmortem for impact and ramp and hold tests. The results showed that the liver tissue became stiffer and more viscous with increased postmortem time. However, it is possible that these changes could have been due to tissue dehydration. Despite the significant change in strain in the current study, the modulus did not change significantly with time for tissue stored in either fluid. However, the modulus has an increasing trend with increased postmortem time for the tissue stored in saline.

It was hypothesized that DMEM would preserve the cellular architecture and material properties more effectively than saline. In a preliminary histology study, Kemper et al. (2013) evaluated the effects at a cellular level of storing bovine liver tissue in DMEM for 24 hours. The histological analysis showed that the DMEM maintained specimen hydration, preserved the cellular architecture, and allowed only mild cell swelling of the parenchyma (i.e., no cell dissociation or nuclear dissolution). This finding was in contrast to a histological analysis performed by Popovic and Simic (1989), in which liver tissue was stored in saline. Popovic

and Simic (1989) observed cellular swelling in guinea pig livers within a few hours postmortem when the tissue was stored in saline. Results from the current study agree with these previous studies. Specifically, three of the six histology samples stored as large blocks in saline revealed relative disruption scores of '2' by the 48 hour time point. Cell swelling was less severe in tissue stored in DMEM than in saline. A relative disruption score of '1'occurred in only one of the livers stored as large blocks in DMEM. However, histology samples were taken from only two of the livers stored as large blocks in DMEM. When the two saline livers showing the least amount of swelling are compared to the two DMEM livers, the relative histology grades are very similar (Figure 33). It is possible that collecting more DMEM histology samples would have resulted in a different trend in histology grades.

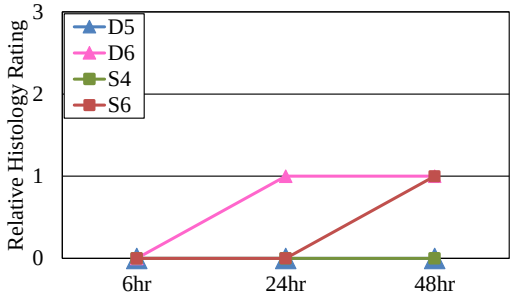

Figure 33: Histology scores from the two saline livers showing the least amount of swelling, and from the two DMEM livers.

The changes in the failure properties with increased postmortem time observed in the liver tissue appear to be related to changes in the cellular structure. This is illustrated by the decrease in failure strain with the increase in disruption rating for tissue stored as large blocks in saline (Figure 18), and for the combined data (Figure 31). Therefore, the lack of change in the failure strain with postmortem time from tissue stored in DMEM is plausibly due to the lower amount of cellular swelling and dissociation. At the cellular level, hepatic

portal structures in human tissue are reinforced by collagen, and sinusoids are supported by thin reticular fibers (Treuting and Dintzis, 2011; Zhang, 1999). Furthermore, a small amount of collagen fibers, fibroblasts, and reticular fibers surround the endothelial cell lining of the central vein (Zhang, 1999). It is possible that cellular swelling and dissociation disrupts this connective tissue, i.e. bindings between adjacent cells and bindings between cells and reticular fibers, and therefore changes the tensile properties. As hepatocytes swell, their outer perimeter changes from a hexagonal shape to a circular shape. This swollen circular shape permits less contact area for bindings between adjacent cells and eventually results in dissociation, i.e., separation between cells. The reduced contact and binding between cells will logically result in lower resistance to separation. However, the suggested disruption of connective fibers and cellular junctions that affect the tensile response may have less effect on the compressive response. Therefore, future studies should evaluate the change in compressive failure properties over postmortem time.

The results of the current study show that storage block size may have an effect on the preservation of the liver's cellular structure and failure properties. Figure 34 shows that the downward trend in failure strain across the time points is more evident for smaller tissue storage sizes. Additionally, the disruption seen at a cellular level is more evident when using smaller tissue storage sizes, as shown in Figure 35. Tissue stored in smaller storage sizes may degrade more quickly because the fluid penetrates more quickly and thoroughly into the tissue. This may result in an earlier and more thorough disruption of connective fibers and bindings between adjacent cells. However, this observation was based on a very limited sample size and no statistical analysis. Furthermore, neither the level of fluid

permeation into the storage tissue blocks nor the condition of blood, e.g., level of hemolysis, were quantified in the current study. Therefore, future studies need to be conducted to further investigate the appropriate tissue storage block size by performing additional tests with matched histology and statistical analyses.

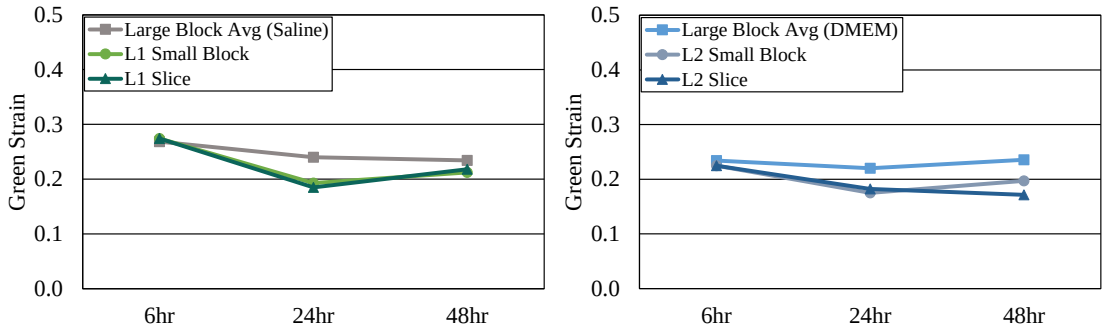

Figure 34: Average failure strain from tissue stored as large blocks, small blocks, and slices in saline (left) and DMEM (right).

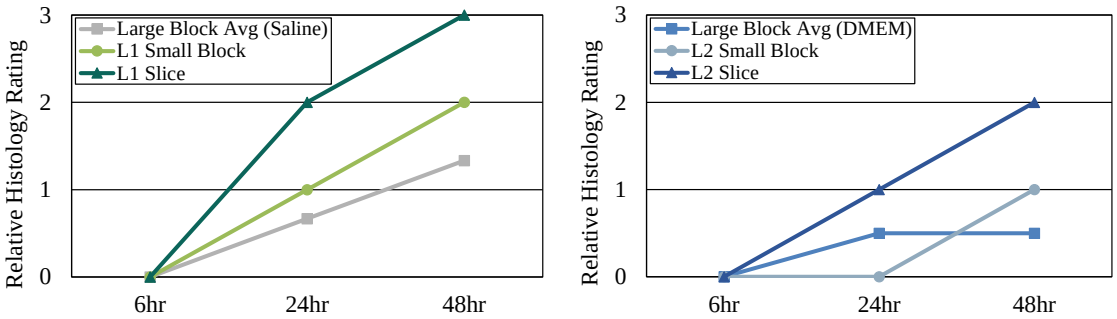

Figure 35: Relative histology ratings from tissue stored as large blocks, small blocks, and slices in saline (left) and DMEM (right).

Limitations

In the current study bovine liver was used as opposed to human liver. This was due to the fact that it is extremely difficult to acquire and conduct tests on human livers within 6 hours postmortem. Previous studies using human livers were only able to test within 36 hours of death (Sparks et al., 2007) and within 48 hours of death (Kemper et al., 2010). Therefore, bovine liver was used as a surrogate for human liver in the current study to conduct testing within 6 hours postmortem. Bovine liver was determined to be an acceptable surrogate for human liver based off of previous studies that have investigated the tensile failure properties of bovine and human liver parenchyma (Kemper et al, 2010; Santago et al., 2009a; Santago et al., 2009b). These studies followed the same methodology used in the current paper and found that the failure properties of bovine liver were comparable to that of human liver (Kemper et al., 2010; Santago et al., 2009a; Santago et al., 2009b). In addition, human and bovine liver are similar at a cellular level. Specifically, the structural arrangement of hepatic lobules are similar. Hepatic lobules are hexagonal arrangements of hepatocytes centered around a central vein. Portal triads are present at each corner of the hepatic lobule and are made up of a bile duct, lymphatic vessel, hepatic artery, and portal vein. Adjacent hepatic lobules in bovine and human liver are not separated by distinct collagenous tissue in the interlobular region (Eurell and Frappier, 2006; Ross and Pawlina, 2011; Zhang, 1999; Henrikson and Kaye, 1986). Conversely, in porcine liver the hepatic lobules are separated by thick layers of collagenous septum (Eurell and Frappier, 2006; Ross and Pawlina, 2011; Zhang, 1999; Henrikson and Kaye, 1986). Furthermore, porcine liver has been shown to have a larger failure stress compared to human liver, and was therefore not used as a surrogate in this study (Uehara, 1995; Kemper et al., 2010).

Variation can be expected during soft tissue material testing due to specimen variability. Detailed procedures were followed in the current study to ensure that each specimen was prepared and tested consistently. These procedures were implemented to minimize the presence of vasculature in the samples. However, some specimen variability is expected due to the fact that liver tissue is not completely homogenous. Parenchyma is made up of hepatocytes and other cells, collagen, arterioles, venules, bile ductules, and lymphatics (Treuting and Dintzis, 2011). The existence of small and/or nonvisible vasculature in a sample is unavoidable and can affect the material response. Also, some samples may have a higher percentage of collagen, depending on the area of the liver the sample was obtained from, that could affect the tissue material response. In order to minimize the effects of specimen variability multiple tests were conducted from each liver at each point. Similarly, six livers were tested for each preservation fluid to ensure that the failure trends over time were consistent and repeatable.

All but two of the animals included in this study were Angus. The one liver from a White Park stored as large blocks, S4, showed the least decrease in strain between 6 and 48 hours postmortem among the livers stored in saline. It cannot be determined whether this was due to the breed type or to subject variation. However, the White Park stored as small blocks and slices (L1) did exhibit a clear decrease in strain across the time points. This may indicate that the unchanging strain response of S4 was likely due to subject variation.

Liver D5 was classified as cirrhotic by the slaughterhouse's inspector. A cirrhotic liver has a high level of fibrosis, or the accumulation of extracellular matrix proteins. Yeh et al.

(2002) found that the severity of fibrosis had a positive correlation with the elastic modulus. However, D5 in the current study had similar failure stress, failure strain, and modulus as the healthy livers. Furthermore, Liver D5 was determined to have a ‘normal’ level of fibrosis according to the veterinary pathologist who graded each histology sample. Therefore, data from D5 was included in the analysis. It is unknown whether the material properties in a cirrhotic liver would be more or less sensitive to the effects of postmortem time. Future studies should evaluate the effects of postmortem time on cirrhotic tissue material properties.

CONCLUSION

Uniaxial tension tests were conducted on bovine liver samples at three time points after death (6hr, 24hr, and 48hr) to quantify the effects of postmortem time on the tensile failure properties and modulus. Tissue was stored in either DMEM or saline to compare the effectiveness of each preservation fluid. Liver tissue was stored as either large blocks, small blocks, or slices, and kept cool between the three time points. A total of 112 dog-bone specimens from twelve bovine livers stored as large blocks were successfully tested. For the two livers stored as small blocks or slices between the time points, 36 tests were completed successfully. The 2nd Piola Kirchhoff stress and Green-Lagrangian strain were calculated for each sample. The average failure stress and strain were then compared for each liver at each of the three time points. There were no significant changes in failure stress or modulus with respect to postmortem time for either fluid. However, there was a significant decrease in failure strain with increased postmortem time for tissue stored as large blocks in saline. Conversely, neither the failure stress nor failure strain changed significantly with respect to postmortem time when stored as large blocks in DMEM. Preliminary results indicated that reducing the tissue storage size had a negative effect on the material properties. Histology samples taken at each time point showed that cellular disruption increased with postmortem time, but the rate and severity of cellular disruption appeared to vary with respect to fluid type and tissue storage size. Specifically, tissue stored in saline generally had more cellular disruption than tissue stored in DMEM for each storage size and time point, and smaller tissue storage sizes generally had more cellular disruption than larger storage sizes for each time point and fluid type. In addition, there was a clear association between an increase in cellular disruption and a decrease in failure

strain. The decrease in failure strain for smaller storage sizes and samples stored in saline was likely due to the fact that the increased cellular swelling and dissociation observed for these samples decreased cell-to-cell bindings and disrupted the connective tissue, thus adversely affecting the tensile properties. Overall, this study illustrated that the effects of postmortem liver degradation varied with respect to the preservation fluid, storage time, and storage block size.

REFERENCES

Brown, J., Rosen, J., Kim, Y., Chang, L., Sinanan, M., Hannaford, B. (2003). In- vivo and in-situ compressive properties of porcine abdominal soft tissues. *Studies in Health Technology and Informatics - Medicine Meets Virtual Reality*, IOS Press, Newport Beach, CA, 26-32.

Brunon, A., Bruyere-Garnier, K., Coret, M. (2010). Mechanical characterization of liver capsule through uniaxial quasi-static tensile tests until failure. *Journal of Biomechanics*, 43, 2221-2227.

Christmas, A., Wilson, A., Manning, B., Franklin, G., Miller, F., Richardson, J., Rodriguez, J. (2005). Selective management of blunt hepatic injuries including nonoperative management is a safe and effective strategy. *Surgery*, 138(4), 606-610.

Chui, C., Kobayashi, E., Chen, X., Hisada, T., Sakuma, I. (2007). Transversely isotropic properties of porcine liver tissue: experiments and constitutive modelling. *Med. Bio. Eng. Comput.*, 45, 99-106.

Eurell, J., and Frappier, B. (2006). *Dellmann's Textbook of veterinary histology* (6th ed.). Ames, Iowa: Blackwell Publishing.

Gao, Z., Lister, K., Desai, J. (2010). Constitutive modeling of liver tissue: experiment and theory. *Annals of Biomedical Engineering*, 38(2), 505-516.

Gayzik, F., Moreno, D., Geer, C., Wuertzer, S., Martin, R., Stitzel, J. (2011). Development of a full body CAD dataset for computational modeling: a multi-modality approach. *Annals of Biomedical Engineering*, 39(10), 2568-2583.

Hardy, W., Howes, M., Kemper, A., Rouhana, S. (2015). In *Accidental injury: Biomechanics and prevention*, ed. N. Yoganandan, A. Nahum, and J. Melvin, pp. 373-434. Springer-Verlag, New York.

Henrikson, R., and Kaye, G. (1986). *Key facts in histology*. New York: Churchill Livingstone.

Holbrook, T., Hoyt, D., Eastman, A., Sise, M., Kennedy, F., Velky, T., Conroy, C., Pacyna, S., Erwin, S. (2007). The impact of safety belt use on liver injuries in motor vehicle crashes: the importance of motor vehicle safety systems. *The Journal of Trauma Injury, Infection, and Critical Care*, 63, 300-306.

Hollenstein, M., Nava, A., Valtorta, D., Snedeker, J., Mazza, E. (2006). Mechanical characterization of the liver capsule and parenchyma. *Proceedings of the Third Int. Conference on Biomedical Simulation*. Springer-Verlag, Berlin, Heidelberg, 150-158.

Huang, Y., King, A., Cavanaugh, J. (1994). Finite element modeling of gross motion of human cadavers in side impact. SAE Technical Paper Series, 942207, 35-53.

Hurtuk, M., Reed, R., Esposito, T., Davis, K., Luchette, F. (2006). Trauma surgeons practice what they preach: the NTDB story on solid organ injury management. *The Journal of Trauma Injury, Infection, and Critical Care*, 61, 243-255.

Jones, C., Tuleuova, N., Lee, J., Ramanculov, E., Reddi, A., Zern, M., Revzin, A. (2009). Cultivating liver cells on printed arrays of hepatocyte growth factor. *Biomaterials*, 30, 3733-3741.

Kemper, A., Santago, A., Sparks, J., Thor, C., Gabler, H., Stitzel, J., Duma, S. (2011). Multi-scale biomechanical characterization of human liver and spleen. In: *22nd International Enhanced Safety of Vehicles Conference Proceedings*, 11-0195.

Kemper, A., Santago, A., Stitzel, J., Sparks, J., Duma, S. (2010). Biomechanical response of human liver in tensile loading. *Ann. Adv. Automot. Med.*, 54, 15-26.

Kemper, A., Santago, A., Stitzel, J., Sparks, J., Duma, S. (2013). Effect of strain rate on the material properties of human liver parenchyma in unconfined compression. *J. Biomechanical Engineering*, 135(10), 104503-1 - 104503-8.

Kerdok, A., Ottensmeyer, M., Howe, R. (2006). Effects of perfusion on the viscoelastic characteristics of liver. *Journal of Biomechanics*, 39, 2221-2231.

Kimpara, H., Nakahira, Y., Iwamoto, M. (2016). Development and validation of THUMS version 5 with 1D muscle models for active and passive automotive safety research. 2016 38th Annual International Conference of the IEEE Engineering in Medicine and Biology Society (EMBC), Orlando, FL, 6022-6025.

Klinich, K., Flannagan, C., Nicholson, K., Schneider, L., Rupp, J. (2010). Factors associated with abdominal injury in frontal, farside, and nearside crashes. *Stapp Car Crash Journal*, 54, 73-91.

Lamielle, S., Cuny, S., Foret-Bruno, J., Petit, P., Vezin, P., Verriest, J., Guillemot, H. (2006). Abdominal injury patterns in real frontal crashes: influence of crash conditions, occupant seat and restraint systems. *Annu. Proc. Assoc. Adv. Automot. Med*., 50, 109-124.

Lizee, E., Song, E., Robin, S., Lecoz, J. (1998). Finite element model of the human thorax validated in frontal, oblique and lateral impacts: a tool to evaluate new restraint systems. *IRCOBI Conference Proceedings*, 527-543.

Lu, Y., Kemper, A., Untaroiu, C. (2014). Effect of storage on tensile material properties of bovine liver. *Journal of the Mechanical Behavior of Biomedical Materials*, 29, 339-349.

Lu, Y., and Untaroiu, C. (2013). Effect of storage methods on indentation-based material properties of abdominal organs. *Proc. Inst. Mech. Eng. H.*, 227(3), 293-301.

Malaki, M., and Mangat, K. (2011). Hepatic and splenic trauma. *Trauma*, 13(3), 233-244.

Mitaka, T., Sattler, G., Pitot, H., Mochizuki, Y. (1992). Characteristics of small cell colonies developing in primary cultures of adult rat hepatocytes. *Virchows Archiv B Cell Pathology*, 62, 329-335.

Na, G., Kim, D., Kim, Y., Han, J., Jung, E. (2014). Effects of glucose concentration in the medium on rat hepatocyte culture. *Ann. Surg. Treat. Res.*, 87(2), 53-60.

Ottensmeyer, M. (2001). *Minimally invasive instrument for in vivo measurement of solid organ mechanical impedence* (Doctoral dissertation). Retrieved from http://hdl.handle.net/1721.1/8858

Pervin, F., Chen, W., Weerasooriya, T. (2011). Dynamic compressive response of bovine liver tissues. *J. of the Mechanical Behavior of Biomed. Materials*, 4, 76-84.

Popovic, D., and Simic, M. (1989). The early post mortem histomorphological changes under experimental conditions. *Acta medicinae legalis et socialis*, 39, 219-226.

Rangarajan, N., Shams, T., McDonald, J., White, R., Oster, J., Hjerpe, E., Haffner, M. (1998). Response of THOR in frontal sled testing in different restraint conditions. *IRCOBI Conference Proceedings*, Sept. 1998, 513-525.

Ross, M., and Pawlina, W. (2010). *Histology: A text and atlas with correlated cell and molecular biology* (6th ed.). Philadelphia: Wolters Kluwer/Lippincott Williams & Wilkins Health.

Rouhana, S., Elhagediab, A., Walbridge, A., Hardy, W., Schneider, L. (2001). Development of a reusable, rate-sensitive abdomen for the Hybrid III family of dummies. *Stapp Car Crash J*. 45, 33-60.

Rouhana, S., Jedrzejczak, E., McCleary, J. (1990). Assessing submarining and abdominal injury risk in the Hybrid III family of dummies: Part II - development of the small female frangible abdomen. In: *34th Stapp Car Crash Conference Proceedings*. SAE paper no. 902317.

Rouhana, S., Viano, D., Jedrzejczak, E., McCleary, J. (1989). Assessing submarining and abdominal injury risk in the Hybrid III family of dummies. In: *33rd Stapp Car Crash Conference Proceedings*. SAE paper no. 892440.

Santago, A., Kemper, A., McNally, C., Sparks, J., Duma, S. (2009a). The effect of temperature on the mechanical properties of bovine liver. *Biomedical Sciences Instrumentation*, 45, 376-381.

Santago, A., Kemper, A., McNally, C., Sparks, J., Duma, S. (2009b). Freezing affects the mechanical properties of bovine liver. *Biomedical Sciences Instrumentation*, 45, 24-29.

Sparks, J., Bolte, J. IV, Dupaix, R., Jones, K., Steinberg, S., Herriott, R., Stammen, J., Donnelly, B. (2007). Using pressure to predict liver injury risk from blunt impact. *Stapp Car Crash Journal*, 51, 401-432.

Stingl, J., Baca, V., Cech, P., Kovanda, J., Kovandova, H., Mandys, V., Rejmontova, J., Sosna, B. (2002). Morphology and some biomechanical properties of human liver and spleen. *Surgical and Radiologic Anatomy*, 24, 285-289.

Tay, B., Kim, J., Srinivasan, M. (2006). In vivo mechanical behavior of intra-abdominal organs. *IEEE Transactions on Biomedical Engineering*, 53(11), 2129-2138.

Tomita, Y., Nihira, M., Ohno, Y., Sato, S. (2004). Ultrastructural changes during in situ early postmortem autolysis in kidney, pancreas, liver, heart and skeletal muscle of rats. *Legal Medicine*, 6, 25-31.

Treuting, P., and Dintzis, S. (2011). *Comparative anatomy and histology: A mouse and human atlas (expert consult)*. Amsterdam: Academic Press.

Uehara, H. (1995). A study on the mechanical properties of the kidney, liver, and spleen, by means of tensile stress test with variable strain velocity. *J. Kyoto Prefect. Univ. Med.*, 104(1), 439-451.

Yeh, W., Li, P., Jeng, Y., Hsu, H., Kuo, P., Li, M., Yang, P., Lee, P. (2002). Elastic modulus measurements of human liver and correlation with pathology. *Ultrasound in Med. & Biol.*, 28(4), 467-474.

Yoganandan, N., Pintar, F., Gennarelli, T., Maltese, M. (2000). Patterns of abdominal injuries in frontal and side impacts. *Annu. Proc. Assoc. Adv. Automot. Med*., 44, 17-36.

Zhang, S. (1999). *An atlas of histology*. New York, NY: Springer-Verlag.